AD

USAAVLABS TECHNICAL REPORT 67-60

FABRICATION AND TESTING OF AN ACTIVE ELECTROSTATIC DISCHARGER SYSTEM FOR THE CH-47 HELICOPTER

By

Juan de la Cierva

David B. Fraser

Paul B. Wilson, Jr.

October 1967

U. S. ARMY AVIATION MATERIEL LABORATORIES
FORT EUSTIS, VIRGINIA

CONTRACT DA 44-177-AMC-114(T)
DYNASCIENCES CORPORATION
BLUE BELL, PENNSYLVANIA

67

Disclaimers

The findings in this report are not to be construed as an official Department of the Army position unless so designated by other authorized documents.

When Government drawings, specifications, or other data are used for any purpose other than in connection with a definitely related Government procurement operation, the United States Government thereby incurs no responsibility nor any obligation whatsoever; and the fact that the Government may have formulated, furnished, or in any way supplied the said drawings, specifications, or other data is not to be regarded by implication or otherwise as in any manner licensing the holder or any other person or corporation, or conveying any rights or permission, to manufacture, use, or sell any patented invention that may in any way be related thereto.

Trade names cited in this report do not constitute an official endorsement or approval of the use of such commercial hardware or software.

Disposition Instructions

Destroy this report when no longer needed. Do not return it to the originator.

DEPARTMENT OF THE ARMY
U. S. ARMY AVIATION MATERIEL LABORATORIES
FORT EUSTIS, VIRGINIA 23604

This report was prepared by the Dynasciences Corporation as a portion of Contract DA 44-177-AMC-114(T). The development of an electrostatic discharger for the CH-47 is outlined, and the equipment is described.

At the direction of the CH-47 project manager and USAAVCOM, this development program was undertaken in late 1963. Laboratory and preliminary flight tests were conducted. Final flight tests which were to be conducted in the arctic environment were terminated short of their completion due to test-aircraft difficulties.

This Command concurs in the conclusions and recommendations presented herein. It is believed that the equipment developed is in keeping with the state of the art that existed at the time of development.

TASK 1F121401A14130
Contract DA 44-177-AMC-114(T)
USAAVLABS Technical Report 67-60
October 1967

FABRICATION AND TESTING OF AN ACTIVE ELECTROSTATIC DISCHARGER SYSTEM FOR THE CH-47 HELICOPTER

Final Report No. DCR 224B

By

Juan de la Cierva
David B. Fraser
Paul B. Wilson, Jr.

Prepared By

DYNASCIENCES CORPORATION
Blue Bell, Pennsylvania

For

U.S. ARMY AVIATION MATERIEL LABORATORIES
FORT EUSTIS, VIRGINIA

SUMMARY

Numerous incidents of severe shock to ground personnel and potential hazards to cargo during external sling load cargo operations have led to extensive research efforts by the U.S. Army Aviation Materiel Laboratories aimed at the dissipation of high electrostatic energy levels present on helicopters. Dynasciences Corporation, in cooperation with USAAVLABS, has fabricated and tested an active electrostatic discharging system for the CH-47 helicopter.

The Model D-03 Electrostatic Discharger is essentially a closed-loop servo system. This report covers its fabrication, mechanical evaluation, environmental testing, and flight testing under both arctic and dusty/high-humidity conditions. Drawings and photographs are included in the report as an aid to a thorough understanding of the system.

FOREWORD

This report was prepared by Dynasciences Corporation, Blue Bell, Pennsylvania, under USAAVLABS Contract DA 44-177-AMC-114(T). The work covered by this report relates to the fabrication and testing of High Performance Active Electrostatic Discharger Systems for helicopters. Mr. Juan de la Cierva was the Dynasciences Corporation Project Manager, and Lts. John Hempstead and Conrad Wall were the cognizant USAAVLABS Project Engineers.

This program was conducted from August 1963 to December 1966. This report was prepared by Juan de la Cierva, David B. Fraser, and Paul B. Wilson, Jr.

The cooperation of the following organizations is gratefully acknowledged:

U.S. Army Aviation Test Board, Fort Rucker, Alabama
U.S. Army Arctic Test Board, Fort Greely, Alaska

TABLE OF CONTENTS

LIST OF ILLUSTRATIONS

INTRODUCTION

The presence of high electrostatic voltages and attendant energies on helicopters creates a hazard to ground personnel and to cargo during external sling load cargo operations. The U.S. Army Aviation Materiel Laboratories has sponsored a substantial amount of research into the dissipation of this electrostatic charge. This research has resulted in a philosophy or design schematic which will satisfactorily dissipate the static electricity from helicopters in certain specified environments (Contract DA 44-177-AMC-3(T)). It was then deemed appropriate that a program be conducted to achieve a system useable by Army helicopters in the field.

The work reported herein relates to the construction and testing of high-performance discharging systems. The performance objectives of this fabrication and test program were (1) the capability of maintaining essentially zero voltage in all charging environments up to 140 microamps, (2) the capability of attaining the zero charging conditions within no more than five seconds after system activation, and (3) the capability of maintaining a helicopter voltage which represents an energy level of one millijoule or less during a hover with the bottom of the fuselage approximately five feet from the ground.

ELECTRONIC DESIGN OF ELECTROSTATIC DISCHARGER SYSTEM

A. SYSTEM DESIGN

The model D-03 Electrostatic Discharger is basically a closed-loop servo control system in which the output is a DC current of positive or negative polarity. The system (Figure 1) consists of a low-voltage unit and two high-voltage units. The low-voltage unit comprises:

a. Sensor mechanism
b. Input amplifier and oscillator printed circuit (PC) board
c. Failure detector PC board
d. Power preamplifier PC board
e. Interconnecting baseboard PC board
f. Cockpit control unit
g. Cargo compartment control unit

The high-voltage unit consists of the following items:

a. Negative high-voltage exciter assembly
b. Positive high-voltage exciter assembly
c. Negative high-voltage multiplier assembly
d. Positive high-voltage multiplier assembly
e. Discharge wicks

A system block diagram is shown in Figure 2 which indicates the order of the elements in the control loop. The electronics circuitry is completely of the solid-state design.

B. LOW-VOLTAGE UNIT, LV02

1. Sensor Mechanism

Refer to the block diagram, Figure 2. As the electrostatic charge builds up on the helicopter, the electrostatic field about the helicopter also increases. The sensor detects the polarity and amplitude of this field and provides the proper signal to an input amplifier. The sensor head (Figure 3) consists of a fixed and a rotating two-bladed vane assembly which acts as a chopper converting the aircraft surface charge into a pulsed current which is easily amplified.

2. Input Amplifier and Oscillator

The input amplifier stage, which is contained on printed circuit board LV02-3 (Figure 4, Sensor, Exposed View), amplifies the output from the sensor mechanism and provides an output signal of sufficient amplitude to activate the dynamic compensator circuit for its proper operation. This amplifier provides the system gain and incorporates the local oscillator used as a carrier signal, which is modulated by the incoming signal. This amplifier also provides the feedback network for controlling system stability. An exposed view showing printed circuit boards in place is shown in Figure 5.

3. Failure Detector

The fail-safe detection logic circuits are located on printed circuit board LV02-4 (Figure 5). These circuits respond to activate the fail lamp when the sensor detects a charge level in excess of the preset safe level for the prescribed aircraft. The fail-safe circuit monitors the output of the sensor input amplifier and indicates, by means of an indicating lamp located in the cargo control unit and cockpit control unit, system performance on a go/no-go basis. The fail-safe circuit will detect any failure of the system other than a failure of the detector itself. This is done as follows:

a. Any failure in the system components in the signal flow prior to the dynamic compensator (including mechanical and/or electrical failures in the sensor mechanisms, input amplifier and fail-safe circuit electronics) will be electrically sensed and will result in a failure indication.

b. Any failure of the system components in the signal flow subsequent to the dynamic compensator (including sensor power output circuits, exciters, multipliers, discharger probes or interconnecting wiring) will result in an aircraft potential exceeding the maximum present with an operative circuit. This aircraft over-voltage will be sensed by the sensor elements, and the signal produced at this point will cause a warning signal to exist in the fail-safe circuit.

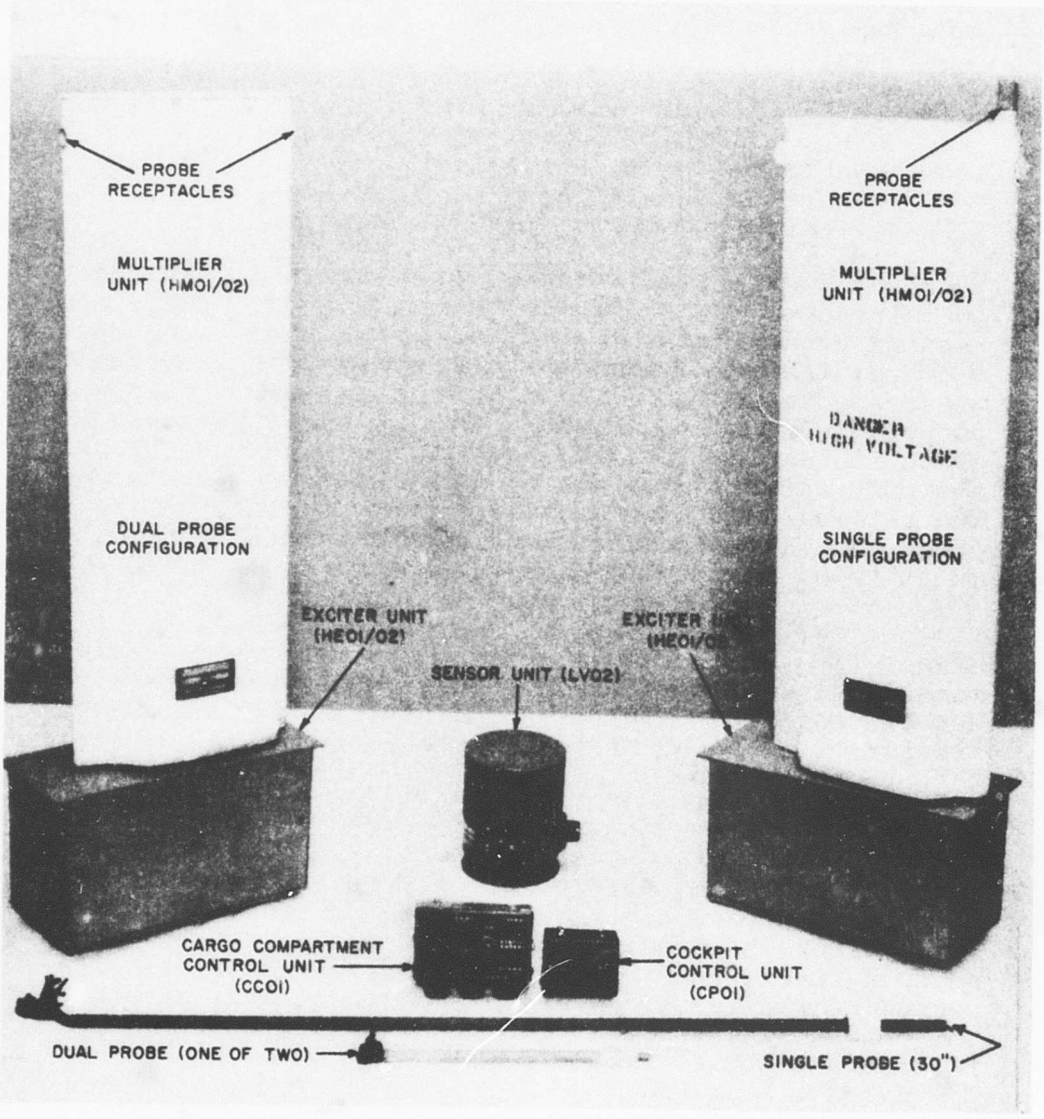

FIGURE 1. MODEL D-03 ELECTROSTATIC DISCHARGER SYSTEM

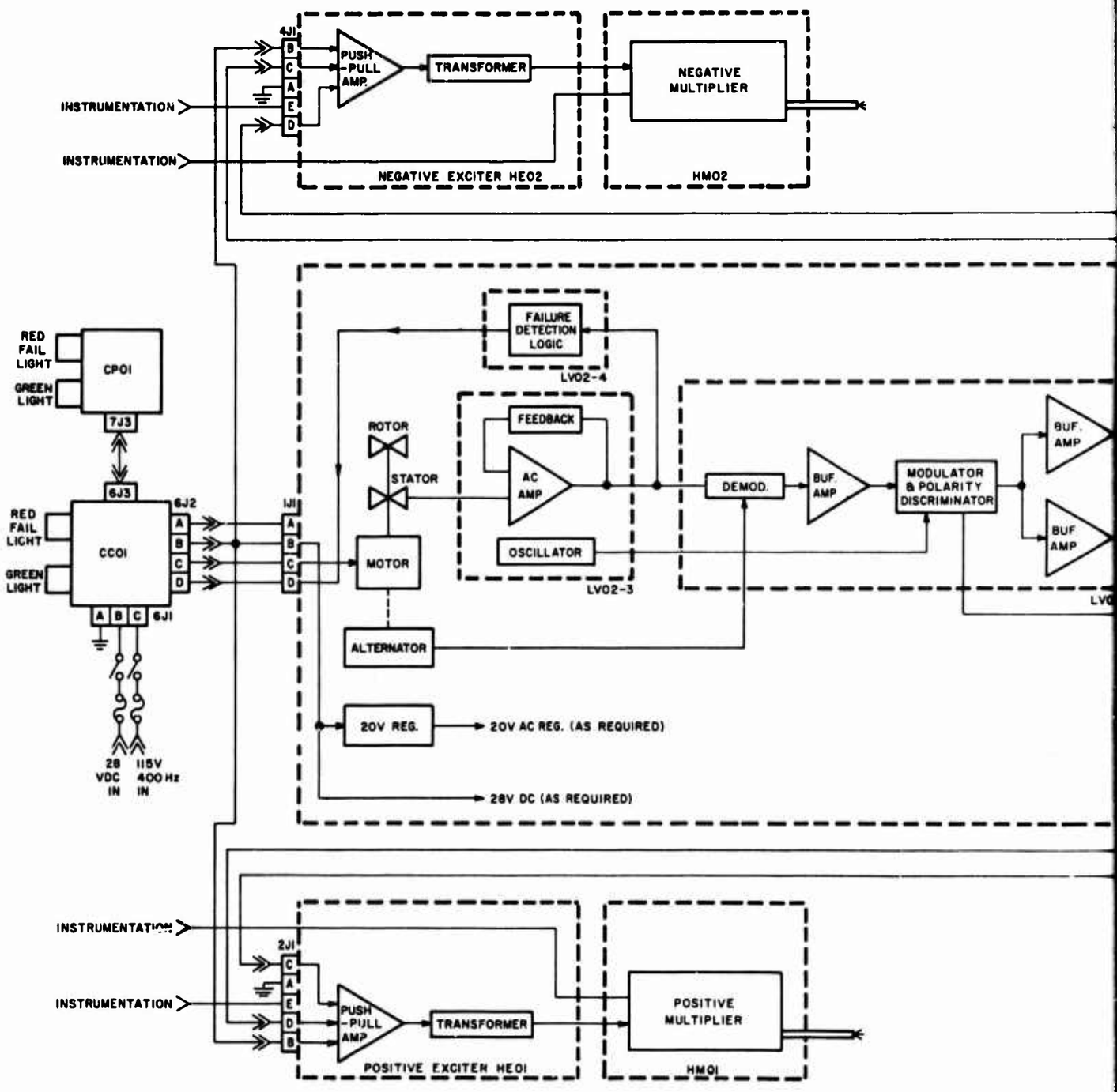

FIGURE 2. SYSTEM BLOCK DIAGRAM

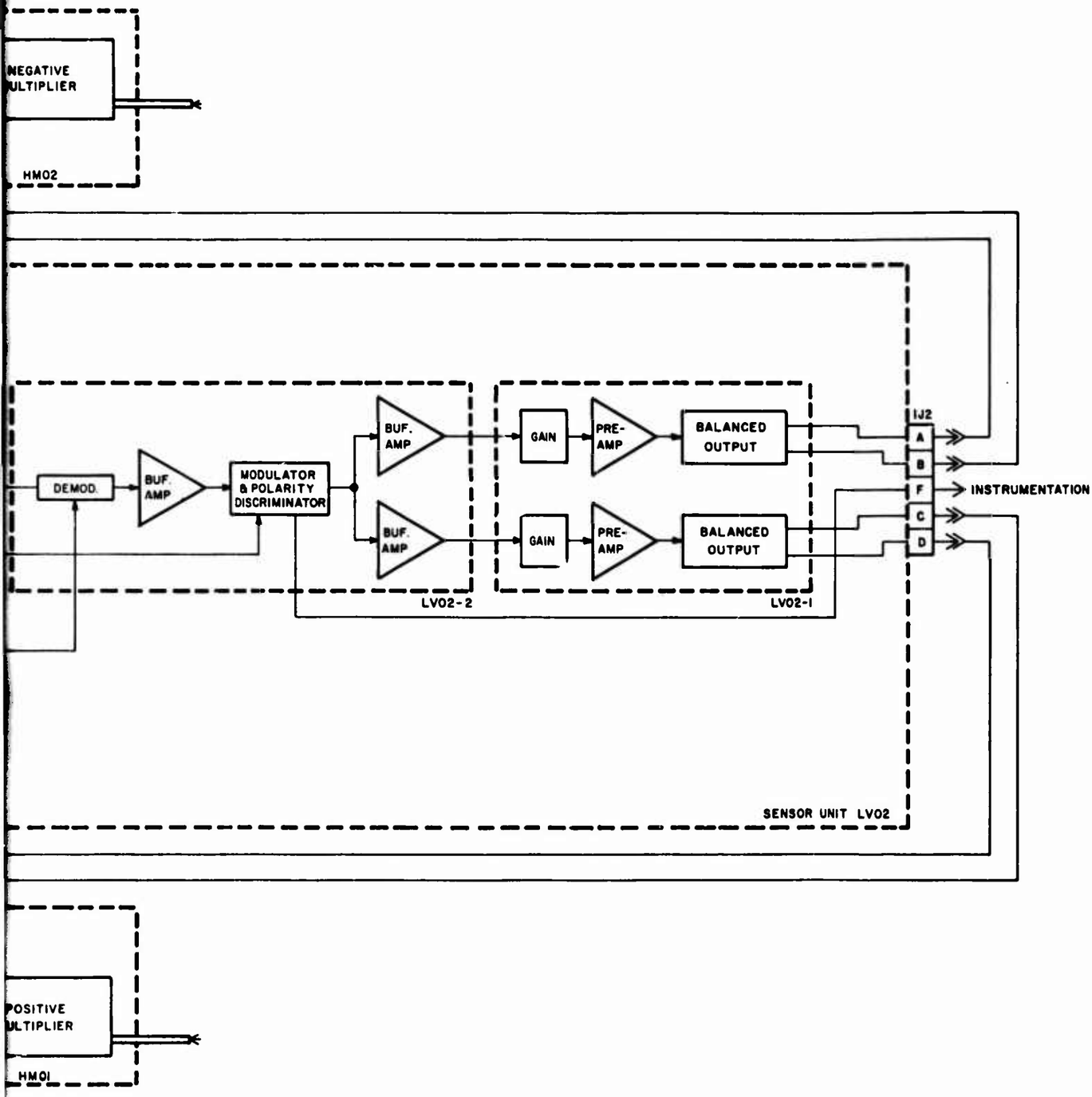
NEGATIVE
ULTIPLIER
HM02
DEMOD.
BUF.
AMP
MODULATOR
& POLARITY
DISCRIMINATOR
BUF.
AMP
BUF.
AMP
LV02-2
GAIN
PRE-
AMP
BALANCED
OUTPUT
GAIN
PRE-
AMP
BALANCED
OUTPUT
LV02-1
IJ2
A
B
F
C
D
INSTRUMENTATION
SENSOR UNIT LV02
POSITIVE
ULTIPLIER
HM01

B

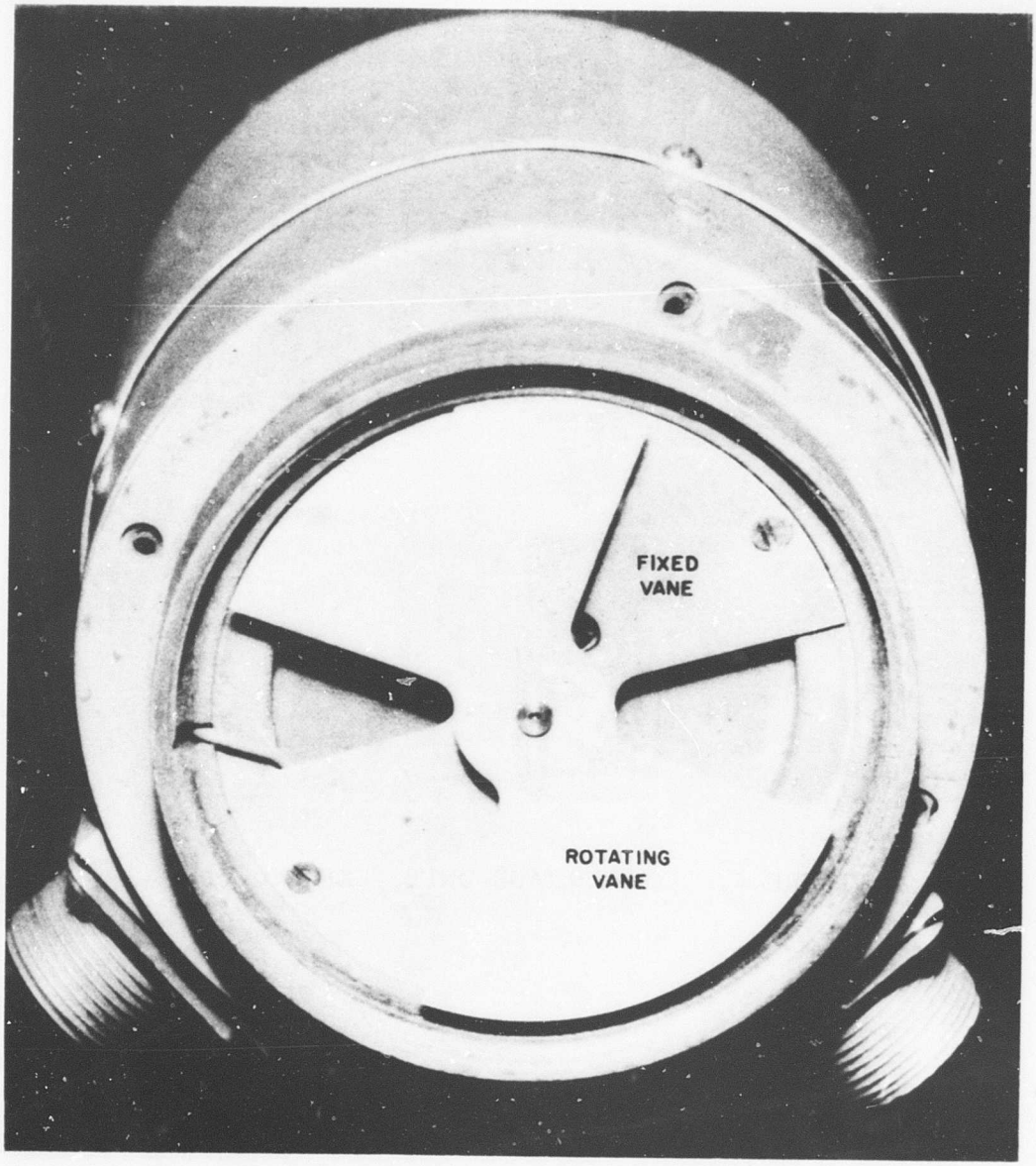

FIGURE 3. SENSOR MECHANISM

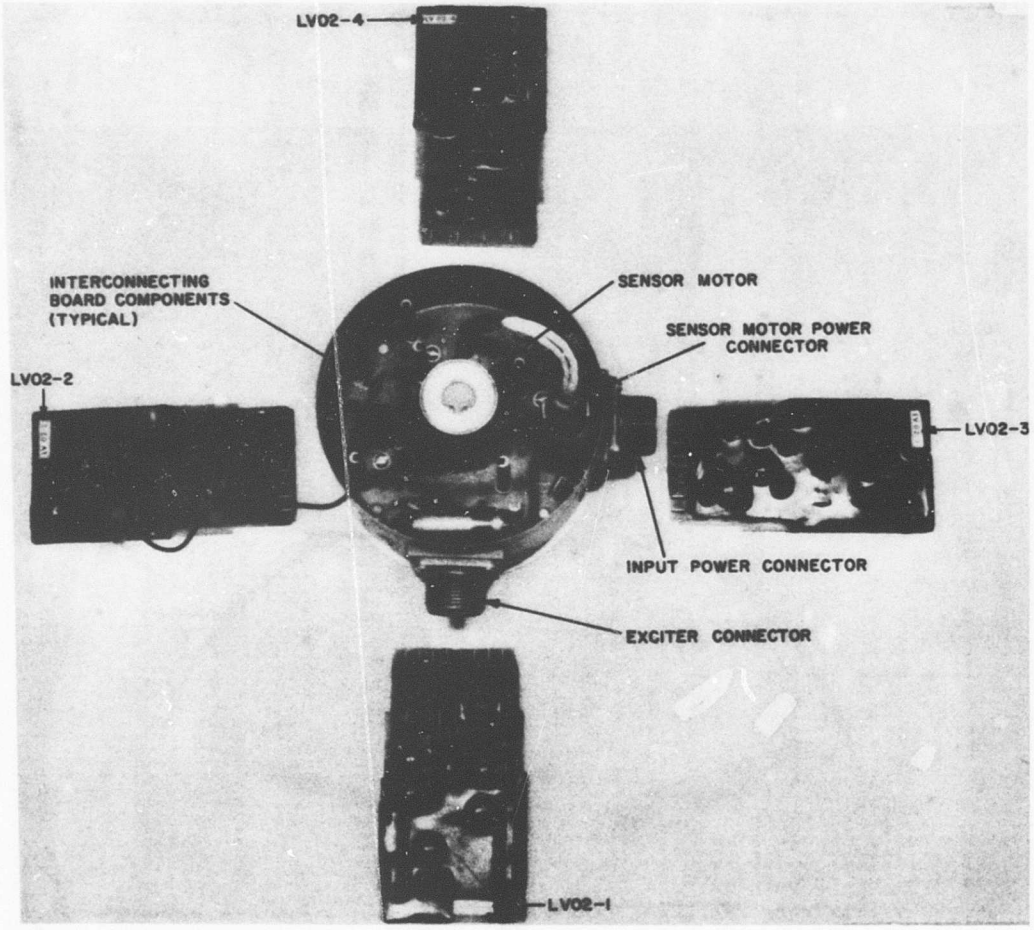

FIGURE 4. LOW-VOLTAGE UNIT, EXPOSED VIEW

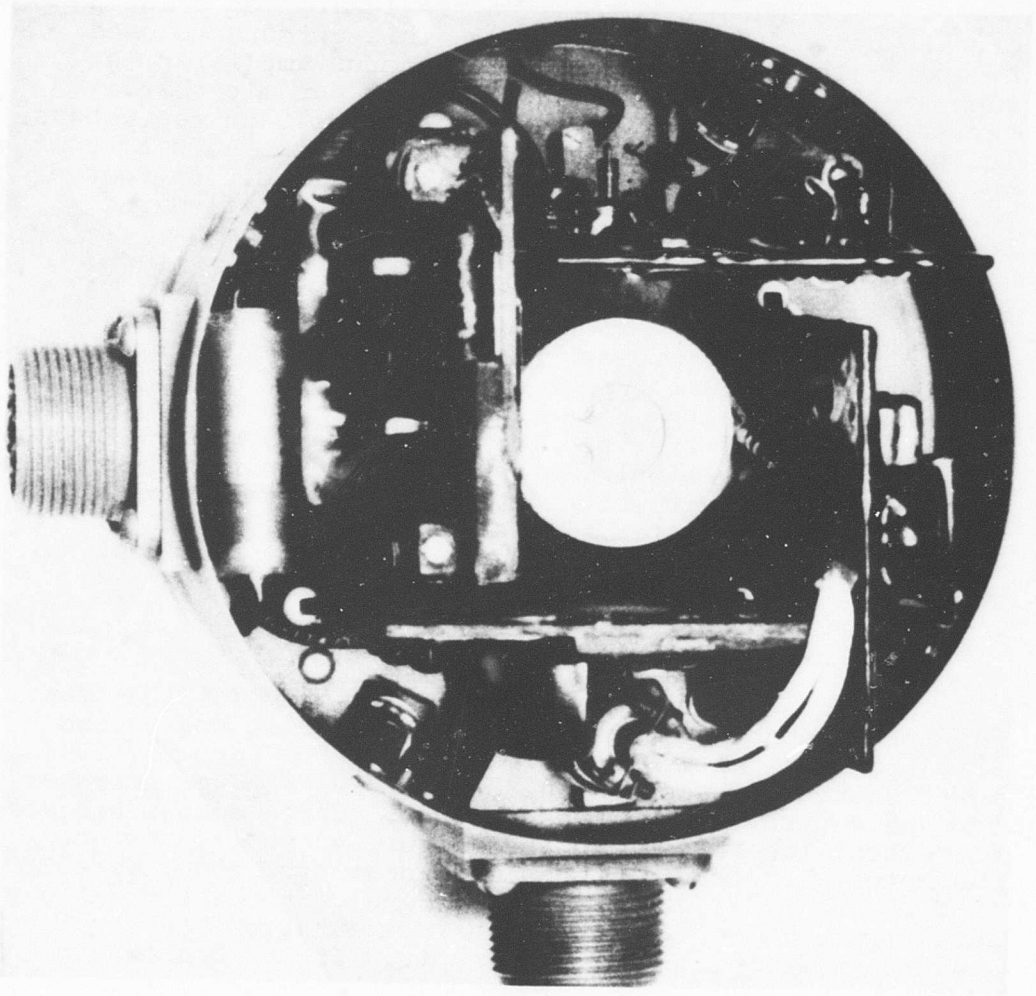

FIGURE 5. EXPOSED VIEW OF SENSOR, PRINTED CIRCUIT BOARDS IN PLACE

4. Dynamic Compensator

The dynamic compensator is located on printed circuit board LV02-2 (Figure 4). This circuit is used to modify the output signal of the input amplifier in such a way as to take into account the dynamic characteristics of the aircraft and the high-voltage generators. The output of the compensator is mixed with the output of the local oscillator and fed to a polarity discriminating network; the appropriate signal is then amplified and becomes the output of this board.

5. Power Preamplifier

The power preamplifier board is located on printed circuit board LV02-1 (Figure 4). The signal input of this board comes from the output of the dynamic compensator board. This amplifier provides the amplification necessary for each of the two polarities separately and the means for controlling the gain which determines the amount of high voltage that the system will generate. This provides the sensor output, which is a balanced and symmetrical signal used for driving the high-voltage unit.

6. Interconnecting Baseboard

The interconnecting baseboard provides the means for interconnecting the four printed circuit boards and also provides the means for regulating the incoming 28V power source and the phasing of the 400 HZ power necessary for the control of the sensor motor. Three connectors are connected with this board (see Figure 4) to (1) connect the motor, (2) provide the power input from the aircraft (28V DC and 115V, 400 HZ) and a signal line to the failure detection lamp and (3) the signal output from the sensor used to drive the high-voltage unit. Figure 6 shows an exterior view of the sensor to depict the exciter connector and the power input connection.

7. Cockpit Control Unit, CP01

The cockpit control unit (Figure 7) contains an ON-OFF switch, a red light and a green light. The red and green lights are controlled by a relay in the cargo compartment control unit.

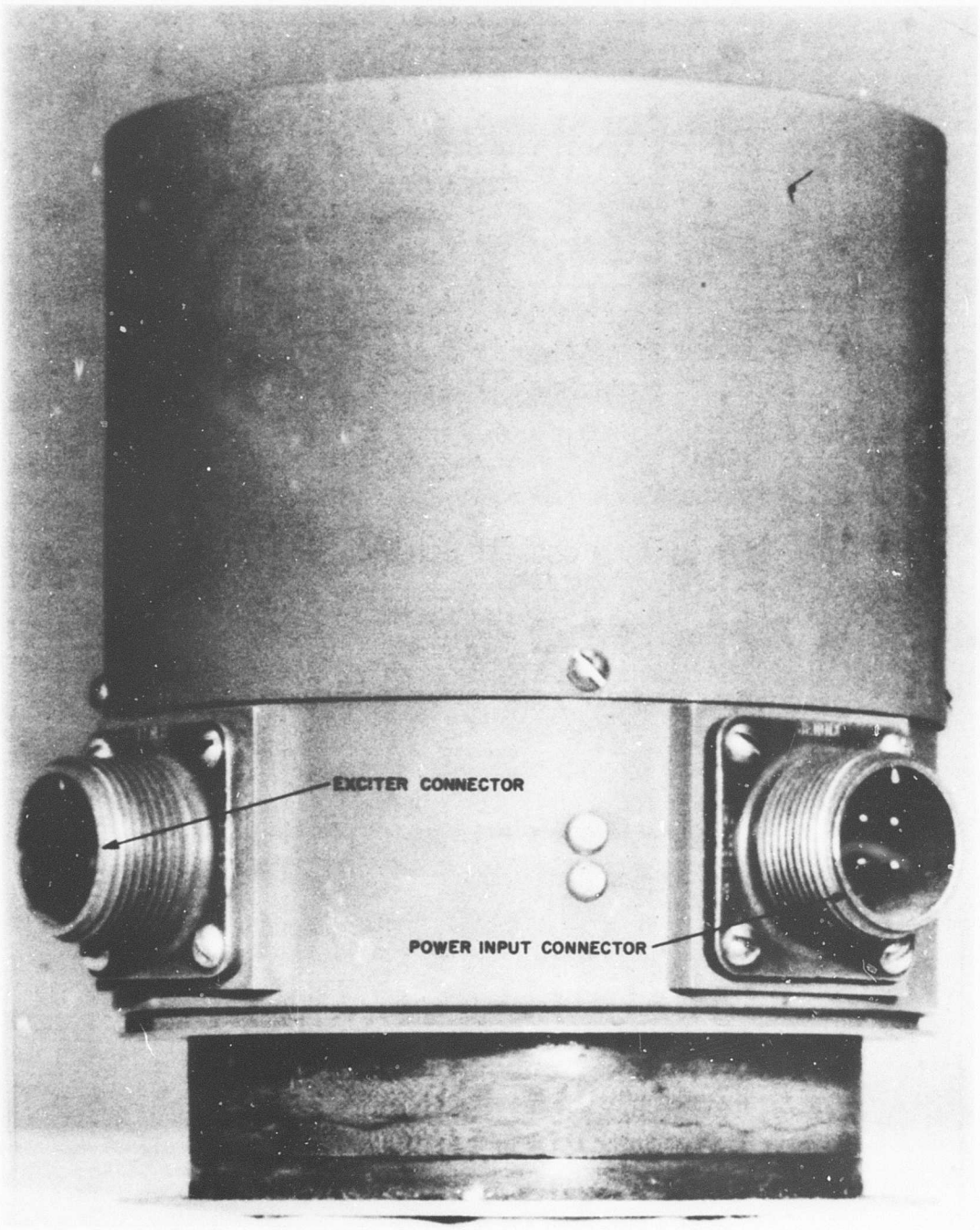

FIGURE 6. SENSOR CONNECTORS

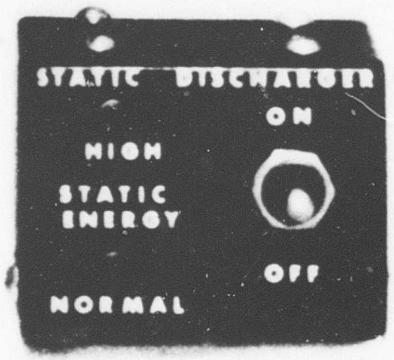

FIGURE 7. COCKPIT CONTROL UNIT

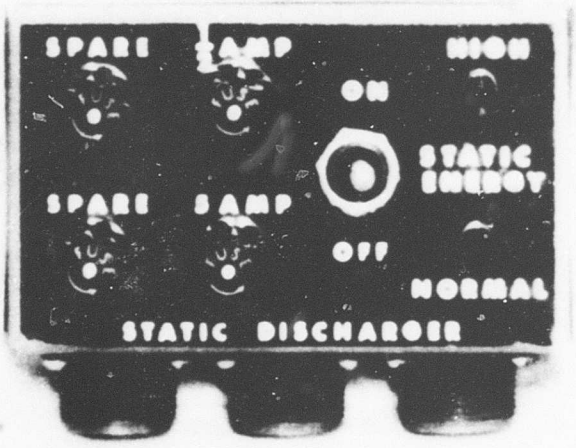

FIGURE 8. CARGO COMPARTMENT CONTROL UNIT

8. Cargo Compartment Control Unit, CC-01

The cargo compartment control unit (Figure 8) provides means to connect the aircraft power to the system. This unit contains the system fuses and the system ON-OFF switch, as well as a red light and a green light. Also contained in this unit is a relay used to activate the green lights when the system is operating normally and to activate the red lights when a malfunction occurs or the charge on the aircraft is excessive (one light of each color in each of the cockpit and cargo compartment control units).

C. HIGH-VOLTAGE UNIT DESIGN

The high-voltage unit (Figure 9) is essentially a balanced emitter-follower power amplifier driving a voltage multiplier unit through a transformer. The multiplier output is terminated in the discharge wick.

1. Exciter Units, HE01 and HE02

The power unit is known as the exciter (Figure 10), HE01 for the positive polarity and HE02 for the negative polarity. The exciter units are identical, HE01 being controlled by the positive sensor output and HE02 by the negative sensor output; they do not operate simultaneously. Each exciter unit is operated independently, being controlled by the polarity discriminator contained within the sensor. The emitter-follower circuit provides the means for current amplification of the signal received from the sensor output. The output of the emitter-follower drives the high-voltage transformer in push-pull and transforms the voltage up to a maximum of 12 kilovolts.

2. Multiplier Units, HM01 and HM02

The HM01 and HM02 multiplier units (Figure 11) are identical except for the direction of the diodes which controls the polarity of the discharge. The multiplier circuit is a classical half-wave rectifier voltage multiplier consisting of six doubler stages (see Figure 11) combined to provide an output voltage up to a maximum of 200 kilovolts. The output of the multiplier terminates in a wick which goes into corona. The ionized air thus created has mass and is blown away by the downwash of the rotor blades and the wind created by the forward motion of the helicopter, thus dissipating the collected charge on the aircraft. The earlier model of the multiplier, with two discharge wicks, is shown in Figure 12. A later model of the multiplier, which terminated in a single discharge wick, is shown in Figure 13.

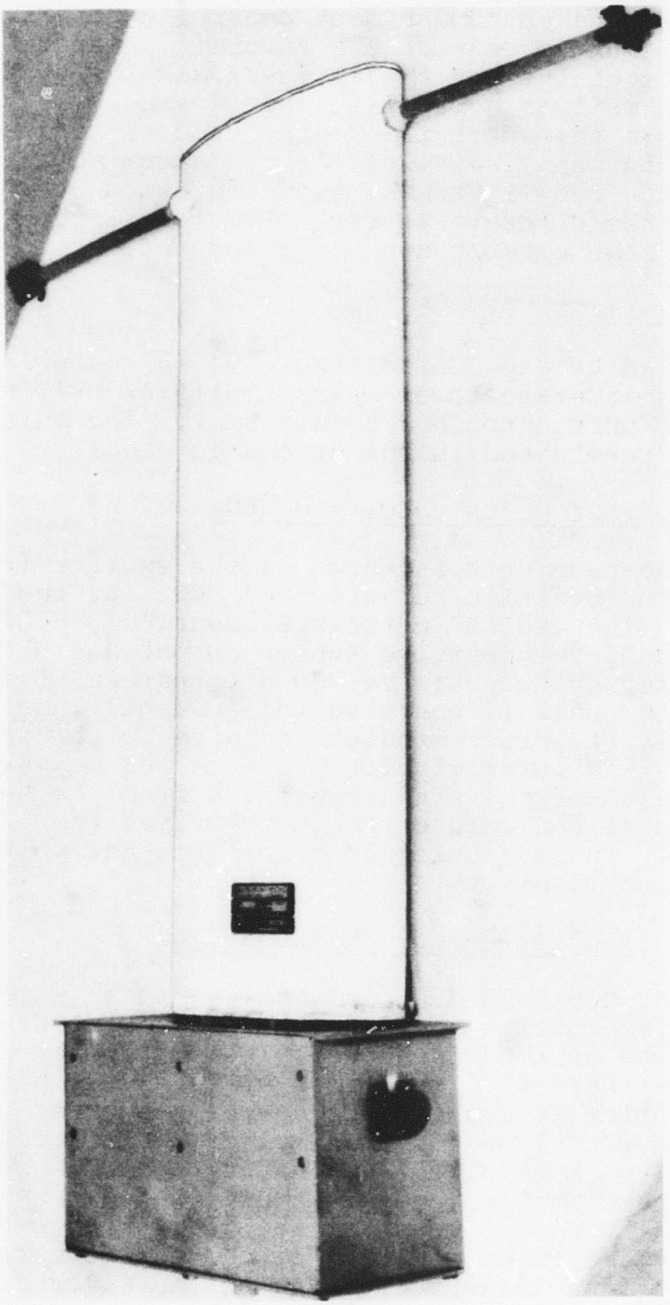

FIGURE 9. HIGH-VOLTAGE UNITS

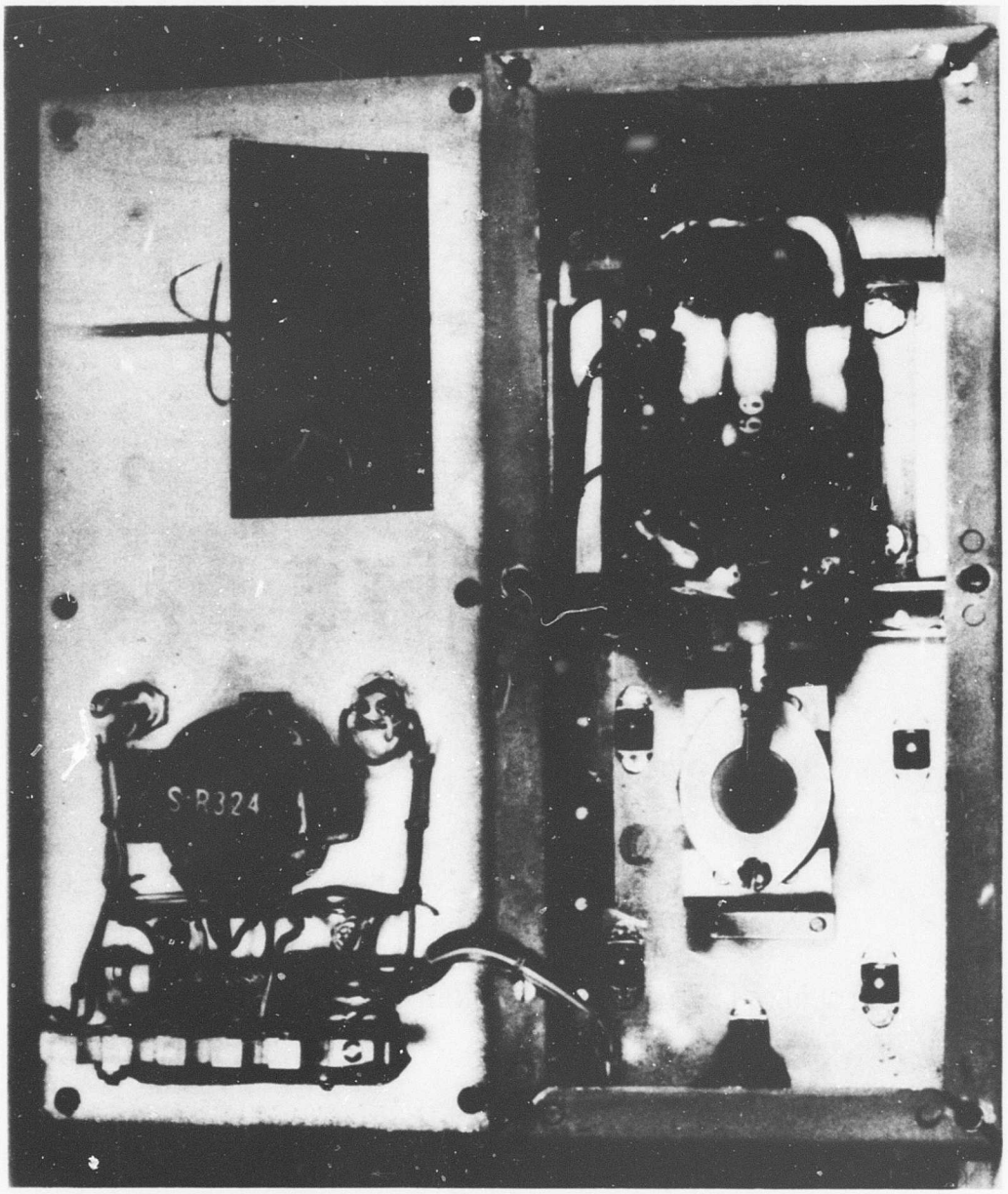

FIGURE 10. EXCITER UNIT

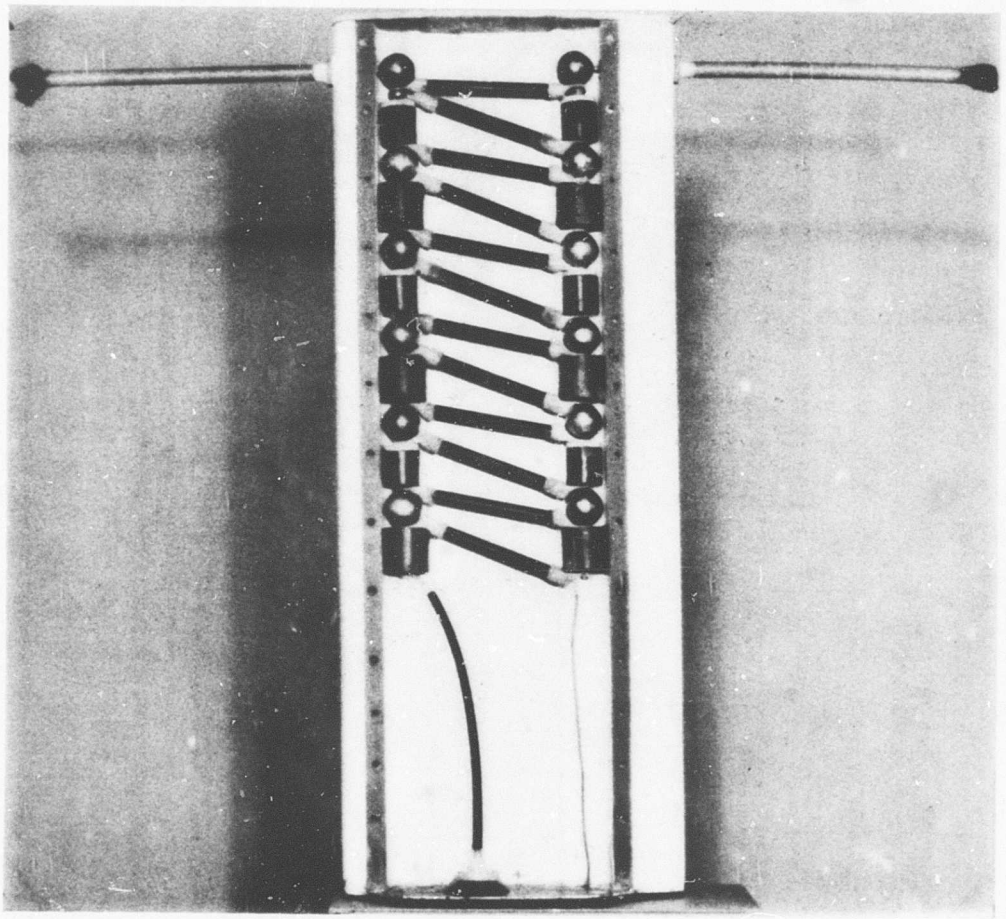

FIGURE 11. MULTIPLIER UNIT (EXPOSED VIEW)

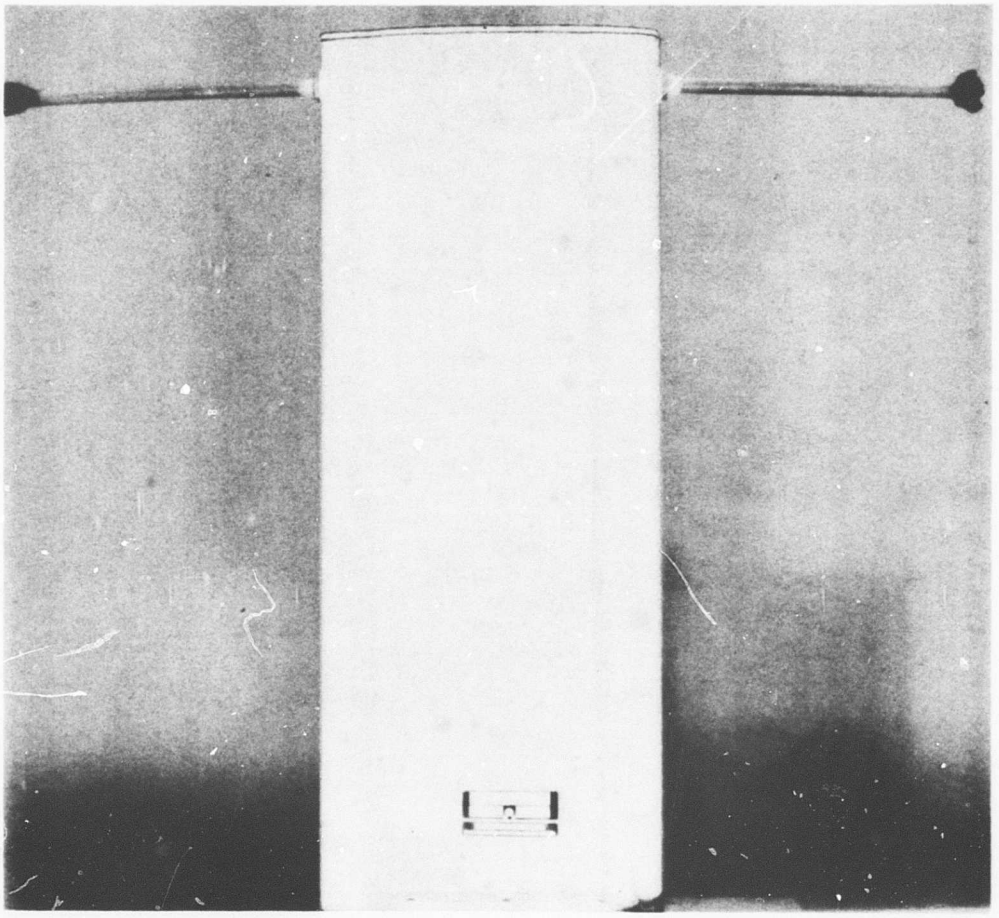

FIGURE 12. EARLIER MODEL OF MULTIPLIER UNIT

FIGURE 13. LATER MODEL OF MULTIPLIER UNIT

STRESS ANALYSIS

This analysis has been conducted to show the capability of the Model D-03 Electrostatic Discharger fairing case to sustain loads imposed upon it when installed on the Chinook helicopter.

The fairing case is fabricated of a plastic laminate, type 181 glass cloth and an epoxy resin. The case cover, fabricated of the same material, is attached to the case with Delrin "500" screws. The assembly is attached to the helicopter with AN bolts located in the root flange area.

The results of this analysis show the 20064549 fairing case to be capable of withstanding the loads imposed when installed on the Chinook helicopter.

A. DESIGN LOAD CRITERIA

The Model D-03 Electrostatic Discharger is designed to meet the following conditions:

Design velocity V_{max} = 130 mph (190.7 ft/sec)

Dynamic pressure q = 43.2 lb/ft^2

Downwash velocity V_R = 90 mph (132 ft/sec)

Assumed airfoil section, NACA 64_3018; reference: NACA Report 824

Maximum angle of attack = 16°

Sectional lift coefficient C_ℓ = 1.2

Maximum assembly weight = 7.5 lb

A factor of safety of 1.0 on the yield and an ultimate factor of safety of 1.5 are applied to all design loads.

B. LOAD ANALYSIS

The 20064549 fairing case, acting as an airfoil, develops air loads and is subjected to "g" loads during landings. The latter are considered to be negligible. It is basically a low-aspect-ratio wing, rectangular in planform and having a symmetrical contour (Figure 14a) approximating that of the NACA 64_3018 airfoil. Detailed coordinates for the fairing airfoil are presented in tabular form in Table I along with those for the NACA 64_3018 section.

(a)

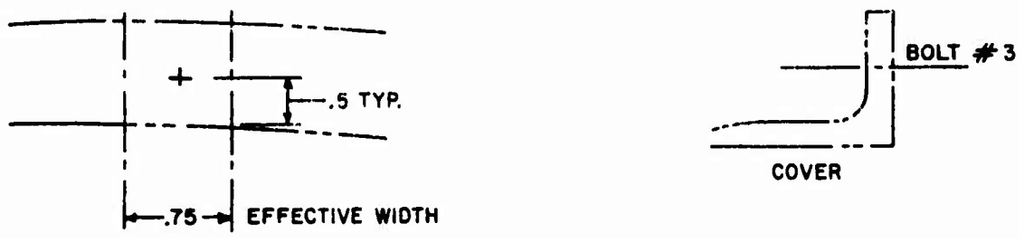

(b)

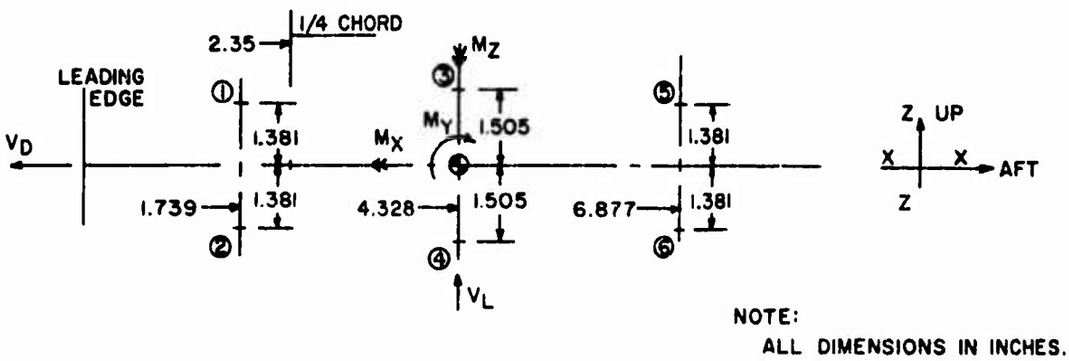

NOTE:
ALL DIMENSIONS IN INCHES.

(c)

FIGURE 14. FAIRING ROOT END LOADS

Design load conditions investigated for the fairing case are:

1. Landing loads @ 4.0 g (negligible)
2. Flight loads @ 130 mph

The loads for these conditions are based on the following:

a. Weight is negligible compared to air loads.
b. The airfoil is at maximum angle of attack at V_{max}.
c. Maximum lift occurs at the quarter chord for a symmetrical section $C_M = 0$.
d. Air load distribution is two dimensional.

TABLE I

FAIRING AIRFOIL COORDINATES
Comparison with NACA 64_3018

Y (in.) Common	20064549 Fairing	NACA 64_3018 Airfoil Ref. NACA Report 824
0.000	0.00	0.000
0.106	0.33	0.205
0.236	0.52	0.283
0.472	0.63	0.395
0.708	0.68	0.480
0.945	0.70	0.549
1.420	0.74	0.656
1.890	0.77	0.736
2.840	0.84	0.831
3.780	0.88	0.845
4.720	0.91	0.766
5.670	0.86	0.630
6.610	0.76	0.456
7.560	0.60	0.273
8.500	0.36	0.095
9.450	0.125R	0.000

C. AIR LOADS-FAIRING

Maximum lift and drag coefficients normal and parallel to the chord at $\alpha_{max} = 16°$ for $V_{max} = 130$ mph are analyzed. See Figure 15.

$$C_L = C_\ell \cos \alpha + C_d \sin \alpha$$

$$= 1.2\ (.9612) + .024\ (.2756)$$

$$C_L = 1.16 \qquad (1)$$

$$C_D = C_\ell \sin \alpha + C_d \cos \alpha$$

$$= 1.2\ (.2756) + .024\ (.9612)$$

$$C_D = -.307 \qquad (2)$$

where

C_L is the lift coefficient, normal to chord
C_ℓ is the lift coefficient
C_D is the drag coefficient, parallel to chord
C_d is the drag coefficient

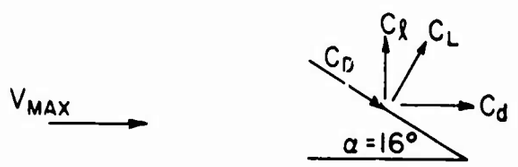

FIGURE 15. VECTOR DIAGRAM OF LIFT AND DRAG COEFFICIENTS

1. Maximum Lift on Airfoil V_L

$$A = \frac{9.4 \text{ in.}}{12 \text{ in.}} (2.0 \text{ ft}), \text{ or } 1.57 \text{ ft}^2$$

$$V_L = q A C_L$$

$$= 43.2 (1.57) 1.16$$

$$V_L = 78.7 \text{ lb (limit)} \quad (3)$$

where

A is the area of the airfoil

2. Maximum Drag V_D Acting Along C_L Chord Due to V_{max}

$$V_D = q A C_D$$

$$= 43.2 (1.57) (-.307)$$

$$V_D = 20.8 \text{ lb acting forward (limit)} \quad (4)$$

3. Maximum Drag Due to Rotor Wake

The fairing is assumed to be a flat plate perpendicular to the flow; reference: Horner, Fluid Dynamics Drag, 1958.

$$C_{Do} = 1.18 \text{ based on frontal area}$$

$$V_{DR} = 1/2 \quad V_R^2 \, C_{Do} \quad A$$

$$= 1/2 (.002378) (132)^2 (1.18) (1.57)$$

$$V_{DR} = 38.2 \text{ lb} \quad (5)$$

where

C_{Do} is the profile drag coefficient
V_{DR} is the vertical load due to downwash (pounds)
is the air density (slugs per cubic foot)

The total vertical load due to downwash V_{DR} and the fairing assembly weight W is:

$$V_{DRT} = V_{DR} + W$$

$$= 38.2 + 7.5$$

$$V_{DRT} = 45.7 \text{ lb} \quad (6)$$

4. Root End Moments Due to Lift and Drag

Refer to Figure 14a.

L = 24 in. (airfoil span)

Root End Moment About X Axis Due to Lift (M_{XL})

$$M_{XL} = 1/2 \; W \; L$$

$$= 1/2 \; V_L L$$

$$= 1/2 \; (78.7) \; (24)$$

$$M_{XL} = 944 \text{ in.-lb (limit)} \quad (7)$$

Root End Moment About Y Axis Due to Lift (M_{XY})

$$M_{YL} = V_L \; d$$

$$= 78.7 \; (1.98)$$

$$M_{YL} = 156 \text{ in.-lb (limit)} \quad (8)$$

Root End Moment About Z Axis Due to Drag (M_{ZL})

$$M_{ZL} = 1/2 \; W \; L$$

$$= 1/2 \; V_D \; L$$

$$= 1/2 \; (20.8) \; (24)$$

$$M_{ZL} = 250 \text{ in.-lb (limit)} \quad (9)$$

5. Root End Mounting Face

The connector loads are determined for the simultaneous application of the lift and drag loads, V_L and V_D, acting on the fairing case. Refer to Figure 14c. Assuming a symmetrical bolt pattern, the applied connector loads tabulated in Table II result.

D. ANALYSIS

The analysis in this section includes the following:

1. Typical Fairing Section
2. Root End Flange
3. Delrin "500" Screws

The materials used in the fabrication are type 181 glass cloth and epoxy resin. The compressive material properties for this laminate are based on published data listed in Table 2-2, page 11 of MIL-HDBK-17, 5 November 1959 for a load angle of 90 degrees.

F_{cy} = 17,900 psi

F_{cu} = 38,200 psi

where

F_{cy} is the allowable compressive yield stress

F_{cu} is the ultimate compressive yield stress

A factor of safety of 1.0 on the yield and an ultimate factor of safety of 1.5 are applied to all limit loads.

1. Section Inertia

The section inertia analysis is based on Figure 16 and Table III.

TABLE II

APPLIED CONNECTOR LOADS

Bolt	1			2			3		
Load	P_x	P_y	P_z	P_x	P_y	P_z	P_x	P_y	P_z
V_L			13.1			13.1			13.1
V_D	3.4			3.4			3.4		
M_x		-78.0			78.0			-170.0	
M_y	-5.5		10.4	5.5		10.4	-6.1		
M_z		-24.3			-24.3			0	
TTL	-2.1	-102.3	23.5	8.9	53.7	23.5	-2.7	-170.0	13.1

Bolt	4			5			6		
Load	P_x	P_y	P_z	P_x	P_y	P_z	P_x	P_y	P_z
V_L			13.1			13.1			13.1
V_D	3.4			3.4			3.4		
M_x		170.0			-78.0			78.0	
M_y	6.1			-5.5		-10.4	5.5		-10.4
M_z		0			24.3			24.3	
TTL	9.5	170.0	13.1	-2.1	-53.7	2.7	8.9	102.3	2.7

$P_z = V_L/6$ $\qquad P_y = \dfrac{M_x\ (z)}{z^2}$ $\qquad P_x = V_D/6$

$P_z = \dfrac{M_y\ (x)}{(x^2 + z^2)}$ $\qquad P_x = \dfrac{M_y\ (z)}{(x^2 + z^2)}$

TABLE II (Continued)

where

x is the horizontal axis distance

y is the lateral axis distance

z is the vertical axis distance

P_z is the vertical load

P_y is the lateral load

P_x is the horizontal load

M_x is the x-axis moment about the bolt centroid

M_y is the y-axis moment about the bolt centroid

M_z is the z-axis moment about the bolt centroid

TABLE III

SECTION MOMENT ARMS

Sect.	d(in.)	d^2(in.^{2})	Sect.	d(in.)	d^2(in.^{2})
1	0.12	0.014	11	0.86	0.740
2	0.25	0.063	12	0.84	0.704
3	0.38	0.144	13	0.83	0.688
4	0.52	0.270	14	0.80	0.640
5	0.63	0.396	15	0.77	0.591
6	0.72	0.519	16	0.73	0.531
7	0.78	0.608	17	0.68	0.462
8	0.82	0.670	18	0.64	0.409
9	0.84	0.704	19	0.48	0.230
10	0.85	0.721			

The section inertia is

$$I = \sum a\, d^2$$

$$= a \sum d^2$$

$$= (a)\ (\sum d^2)$$

$$= (0.5 \times .063)\ (18.2)$$

$$I = 0.573 \text{ in.}^4 \qquad (10)$$

where

I is the section inertia
a is the section area (from Figure 16)
d^2 is the square of the moment arm of a section segment

We also note that:

A_{case} = area of case = 0.772 in.^{2}

A_{cover} = area of cover = 0.463 in.^{2}

d_{avg} = centroid of cover area = 0.762 in.

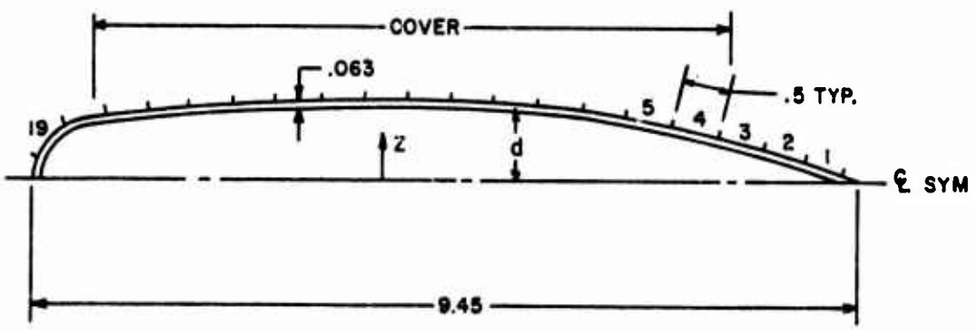

FIGURE 16. ASSUMED EFFECTIVE SECTION

2. Section Stress

The maximum limit stress in a typical airfoil section, assuming the maximum spanwise moment is applied, is analyzed. Stress due to drag force is considered to be negligible.

$C = .89$ in.

$$f_b = \frac{MC}{I} = \frac{M_{XL}\, C}{I}$$

$$= \frac{944(.89)}{.573}$$

$$f_b = 1174 \text{ lb/in.}^2 \text{ (limit)} \qquad (11)$$

$$f_{bu} = 1174\ (1.5)$$

$$f_{bu} = 2211 \text{ lb/in.}^2 \text{ ultimate}$$

F_c allowable 17,900 psi (Reference: Table 2-2, page 11 of MIL-HDBK-17, 5 November 1959)

$$MS = \left(\frac{f_{bu}}{F_c} = 1\right) \geq 2 \qquad (12)$$

where

f_b is the applied bending stress

M is the applied moment

C is the distance from the section centroid to the outermost fiber

f_{bu} is the ultimate bending stress

F_c is the ultimate allowable compressive stress

MS is the margin of safety

3. Delrin Screws

The maximum limit shear stress in the Delrin screws attaching the cover to the case is calculated. Shear loads result from a change in moment along the span of the fairing. See Figure 17.

The screws, loacted 2.47 inches from the mounting face, carry the shear developed between the face and the location 3.42 inches outboard, which is centered between the two inboard screws.

M Due to Change in Shear

$$w = \frac{V_L}{L}$$

$l = 20.58$ in. (see Figure 17)

$$M = M_{XL} - \tfrac{1}{2} w l^2$$

$$= 944 - \frac{3.28\ (20.58)^2}{2}$$

$$M = 252 \text{ in.-lb (limit)} \qquad (13)$$

where

w is the load per inch

a. Shear Load in Screws

$$P_1 = \frac{M\ d_{avg}\ A_{cover}}{21}$$

$$P_1 = \frac{252}{2} \quad \frac{.762\ (.463)}{.573}$$

$$P_1 = 77.6 \text{ lb (limit)} \qquad (14)$$

where

P_1 is the shear load of screws

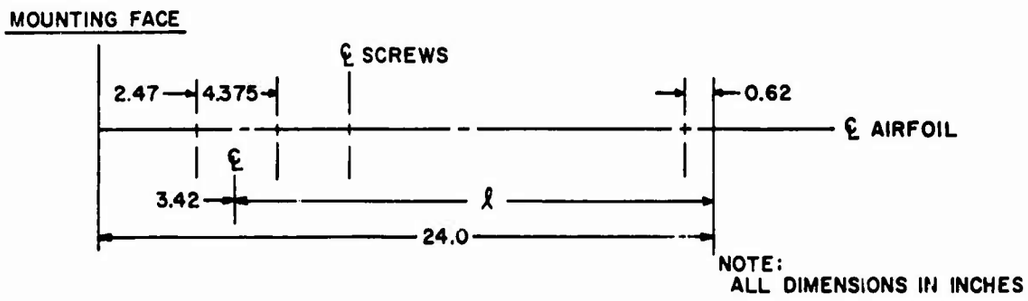

FIGURE 17. PARAMETERS AFFECTING DELRIN SCREW STRESS

Thus a screw size #10-24 with a minimum thread diameter of 0.1359 in. and a screw area A_s of .0147 $in.^2$ is required.

b. Shear Stress in Screws

$$f_s = \frac{P_1}{A_s}$$

$$= \frac{77.6}{.0147}$$

$$f_s = 5280 \text{ lb/in.}^2 \text{ (limit)} \quad (15)$$

$$f_{sult} = 1.5 f_s$$

$$= (1.5)(5280)$$

$$f_{sult} = 7920 \text{ lb/in.}^2 \quad (16)$$

$$F_{savg} = 9500 \text{ lb/in.}^2 \text{ (average value)*}$$

Reduce F_{savg} by 15% for shear allowable

Thus

$$F_s \text{ allowable} = F_{savg} (1-.15)$$

$$= 9500 (1-.15)$$

$$F_s \text{ allowable} = 8070 \text{ lb/in.}^2 \quad (17)$$

$$MS = \frac{8070}{7920} - 1, \text{ or } 2\% \quad (18)$$

where

f_s is the shear stress in screws

f_{sult} is the ultimate shear stress in screws

F_{savg} is the average allowable shear stress in screws

MS is the margin of safety

*Anon, Plastics Catalog, Plastics Center, Inc., 228-230 North 15th Street, Philadelphia, Pennsylvania, 1963.

4. Root End Connection

The assumed effective section of the flange in bending is b = .75 inch. Refer to Figure 14b. The nominal flange thickness (cover) is t = .25 inch. Refer to Figure 14c.

Flange Bending

$$f_b = \frac{MC}{I}$$

$$= \frac{6P_y(.50)}{bt^2}$$

$$= \frac{6(170)\ (.5)}{.75\ (.25)^2}$$

$$f_b = 10{,}880\ \text{lb/in.}^2 \text{(limit)} \qquad (19)$$

$$f_{bult} = 1.5\ f_b$$

$$= (1.5)\ (10{,}880)$$

$$f_{bult} = 16{,}300\ \text{lb/in.}^2 \qquad (20)$$

where

f_{bult} is the ultimate bending stress

Shear

$$f_s = \frac{P_y}{A}$$

$$= \frac{170}{(.75)\ (.25)}$$

$$f_s = 906\ \text{lb/in.}^2 \qquad (21)$$

F_c Ultimate = 17,900 lb/in.^{2} (Reference: Table 2-2, page 11 of MIL-HDBK-17)

$$MS = \frac{17900}{16300} - 1 = 10\% \qquad (22)$$

ENVIRONMENTAL TESTING

Environmental tests were performed by an independent test laboratory, American Electronics Laboratory* (AEL). These tests provided the essential data necessary for design improvements to prevent failure of the system under extremes of flight conditions. Tests were performed in accordance with Military Specification MIL-E-5272C. A brief summary of the tests performed are given in the sections that follow. However, greater detail may be obtained by a study of the AEL report.

A. PROCEDURES FOLLOWED

During the course of environmental testing, operation of the system was monitored by predetermined measurements. The test procedures used to verify system performance are included as an appendix to this report. These procedures were established for use as a standard for comparison during the tests made by AEL. The environmental tests conducted included the following:

1. Temperature-humidity-altitude
2. Shock, vibration, and acceleration
3. Sand and dust
4. Explosion
5. Rain and salt spray
6. Fungus

Performance tests included the monitoring of discharge current, sensor voltage, and helicopter voltage.

B. INTERMEDIATE TEST RESULTS

After each environmental test, system performance records were evaluated and each unit was inspected to determine whether modifications were required. The results of these tests are summarized in the following discussion.

* American Electronics Laboratory Report No. 6401704, "Aircraft Static Discharger Under Simulated Environmental Conditions for Dynasciences Corporation", AEL Environmental and Measurements Laboratory, Colmar, Pennsylvania.

A low-temperature test was performed with the equipment first stored at -62 degrees centigrade and then operated at -54 degrees centigrade. Modifications necessary for the cargo compartment control unit and the sensor unit as a result of these low temperatures are delineated in Section C. With these modifications made, electrical operation of the system at low temperature was satisfactory. Visual inspection revealed no physical or mechanical damage to any of the units.

The units were vibrated over a range of 5 to 2000 HZ with a force of 10g. Minor modifications were made in the cargo compartment control unit as a result of the loosening of some components. These modifications will be discussed in Section C. No other physical or mechanical damage was noted in any of the units. Electrical operation was checked and found to be satisfactory.

The system was subjected to a physical shock of 15g with a shock pulse width of 11 milliseconds, in each of three mutually perpendicular planes. No evidence of mechanical damage was noted and satisfactory electrical operation was obtained.

The system was operated at a temperature of +71 degrees centigrade. Satisfactory electrical operation was obtained. No evidence of mechanical damage was noted as a result of this test.

The system was placed in the test chamber, and the chamber temperature was lowered to -54 degrees centigrade, after which the chamber pressure was reduced to simulate an altitude of 50,000 feet. Initial attempts to operate the equipment were hindered by a deficiency in the cable harness which was adjudged not to be due to environmental testing. After correction of this deficiency, a satisfactory performance test was made. No evidence of mechanical damage was noted as a result of this test.

A complete sequence of temperature and altitude conditions, induced at the maximum rates permissible by the test chamber, was performed with the discharger system alternately being stored, then operated. Temperatures were monitored by means of thermocouples attached to the units and by means of thermocouples suspended within the chamber to measure the ambient temperature. Proper electrical operation was obtained throughout the test where operation was required. No evidence of physical or mechanical damage was noted as a result of these tests.

An acceleration test in which a force of 14g was applied along each of three mutually perpendicular planes was performed with the system in a nonoperating condition. No evidence of mechanical damage was noted as a result of acceleration. Satisfactory electrical operation was obtained following the test.

A humidity test was performed with a range of temperatures from +28 degrees to +71 degrees centigrade at a relative humidity of 95 percent and with the system in a nonoperating condition. After a total of 240 hours of exposure to the humidity conditions, covers and connections to each unit were removed and these areas were wiped dry. Wicks on the multiplier units were dried. A satisfactory electrical performance test was conducted. Visual inspection revealed the advisability of modifications to prevent minor corrosion in some areas.

The explosion test was performed with the exclusion of the multiplier units and discharge wicks, as it was assumed that these units would be mounted external to the aircraft. Operation of the rest of the units or their switches did not cause the chamber's gasoline vapor atmosphere to explode at any of six test altitudes. Test altitudes were simulated up to 50,000 feet. No impairment of operation or mechanical damage was noted as a result of electrode detonation of the explosive mixture.

Sand and dust conditions were induced with a density of 0.1 to 0.5 gram per cubic foot at a velocity between 2000 and 3000 feet per minute. Sand and dust used in the test were of angular construction and were of such size that 100 percent could pass through a 100-mesh screen and 75 percent could pass through a 325-mesh screen. Multiplier units and discharge wicks only were subjected to this test since they are the only units exposed to these conditions. No evidence of mechanical damage or of penetration of sand or dust into the interior of the units was noted. Proper operation of the units was obtained following the test.

Rain conditions were introduced in the chamber with a simulated rainfall of 4 ± 1 inches per hour produced in droplets having a minimum diameter of 1.5 millimeters. Temperature of the water was controlled between 11 degrees and 20 degrees centigrade. Only multiplier units and discharge wicks were subjected to this test since they are the only units exposed to these conditions. No water leakage to the interior of the units was noted. Equipment operated properly following this test.

All units of the system were placed in the chamber and sprayed with a suspension of mixed spores of fungi of the species required in MIL-E-5272C. The ambient conditions of the chamber were maintained at a temperature of 30 degrees centigrade and a relative humidity of 95 percent. The system was not operated following this test. Visual examination revealed peeling of paint from some of the units. Corrosion was noted on external surfaces of the units and on various parts and components of the cargo compartment control units. Fungus growth was observed, particularly where insertion and withdrawal of printed circuit boards had removed protective coating. These results suggested necessary improvements to protective coatings of the units.

A 20-percent salt solution was sprayed indirectly (in accordance with Federal Test Methods Number 151, Method 811) on externally exposed parts and surfaces of the system. The units were subjected to this condition for a period of 168 hours. No evidence of corrosion, pitting of materials, or peeling of painted or coated surfaces was noted.

C. MODIFICATIONS RESULTING FROM TESTS

Electronic circuit design changes consisting of capacitors with proper temperature coefficients were installed in the cargo compartment control unit and sensor unit to compensate for malfunctions as a result of low-temperature conditions. Seals were modified in applicable units to prevent moisture due to humidity from affecting system operation.

The capacitor and transistor in the cargo compartment control unit which had broken loose during the vibration test were replaced, and permanence was insured by coating these components with an epoxy.

As a result of the fungus tests, nonnutrient materials were substituted for those affected by fungus growth. In addition, the printed circuit boards were encapsulated to provide protection from fungus and vibration.

D. FINAL TEST RESULTS

After modification of the units involved, performance tests were run to assure proper operation. The system performed satisfactorily in accordance with the test specifications.

FLIGHT TESTING

A. FORT RUCKER, ALABAMA

The discharger system was first flight tested at Fort Rucker; these tests were performed during the period from November 1963 to January 1964.

1. Aircraft Installation

Installation of the system is illustrated in Figure 18. The multiplier and exciter units were installed approximately at midsection. Mounting of the multiplier units required the stiffening of the frame at midspan to eliminate possible torsional twisting.

The flight test instrumentation setup is shown in Figure 19. The original version of the discharger test set, TS-16, is shown in Figure 20.

A stress analysis was conducted for the exciter and multiplier units and is summarized in Table IV. The stresses developed allow the margin of safety indicated, based on static loading.

TABLE IV

SUMMARY OF STRESS ANALYSIS RESULTS

ITEM	MARGIN OF SAFETY
Fairing Mounting Flange	0.1
Mounting Bolts	6.0
Fairing Cover Screws	0.02
Exciter Unit-Fairing Connection	1.6
Exciter Unit Mounting Bolts	18.0
Exciter Unit Plate Nut Rivets	4.0
Fairing Case	8.0

A detailed stress analysis of the fairing case is included in the section entitled "Stress Analysis".

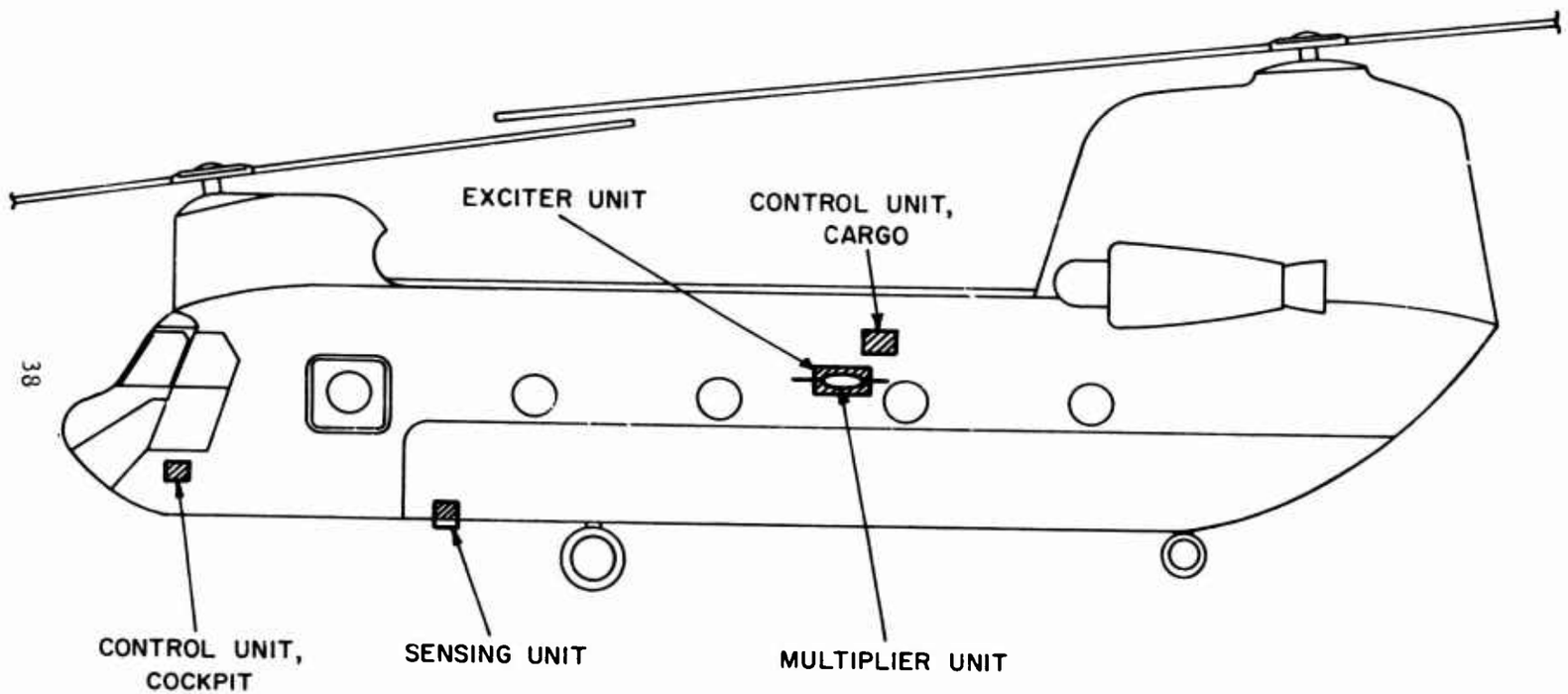

FIGURE 18. AIRCRAFT INSTALLATION

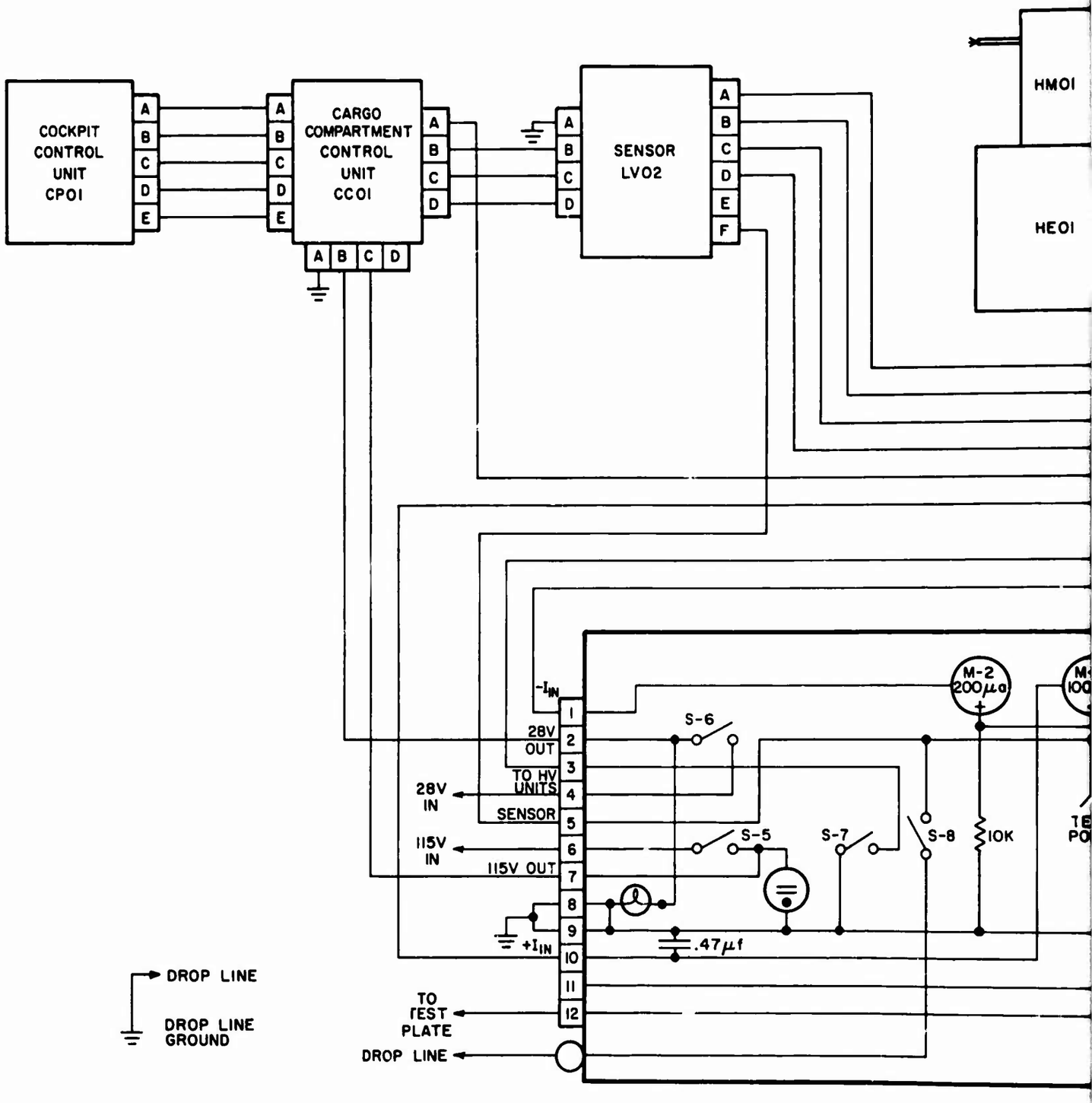

FIGURE 19. FLIGHT TEST SETUP

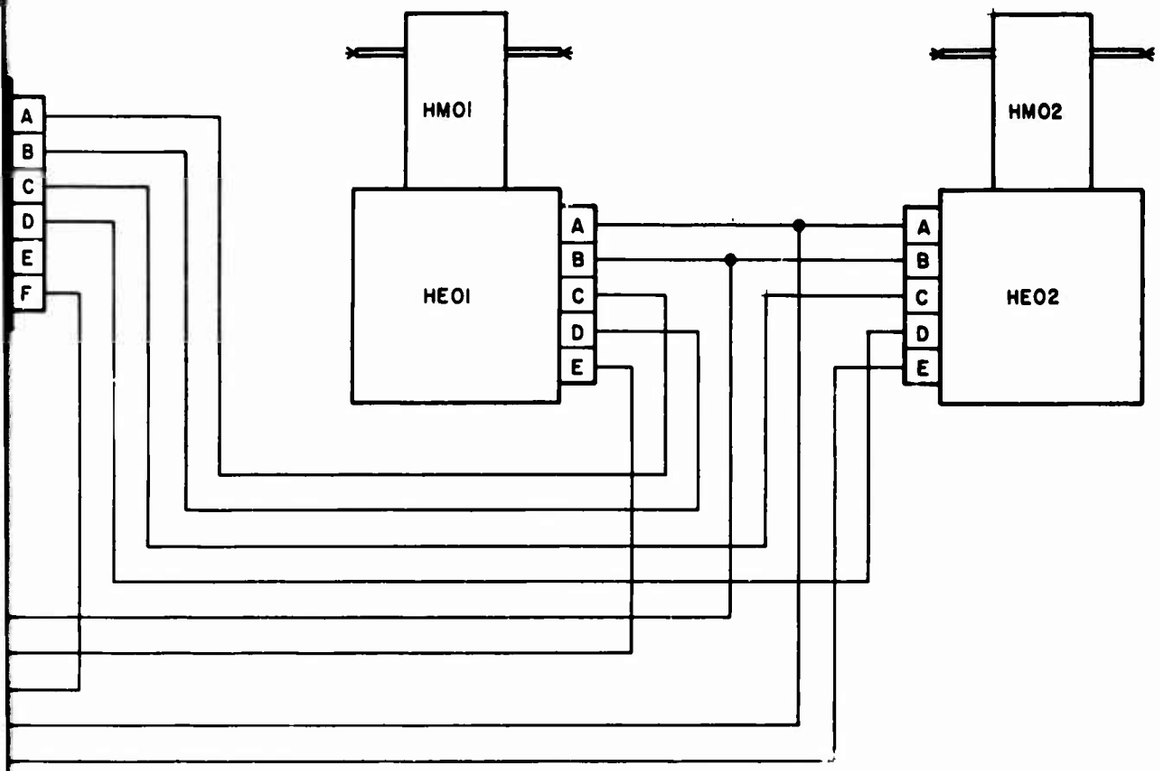
HM01
HM02
HE01
HE02
A
B
C
D
E
F

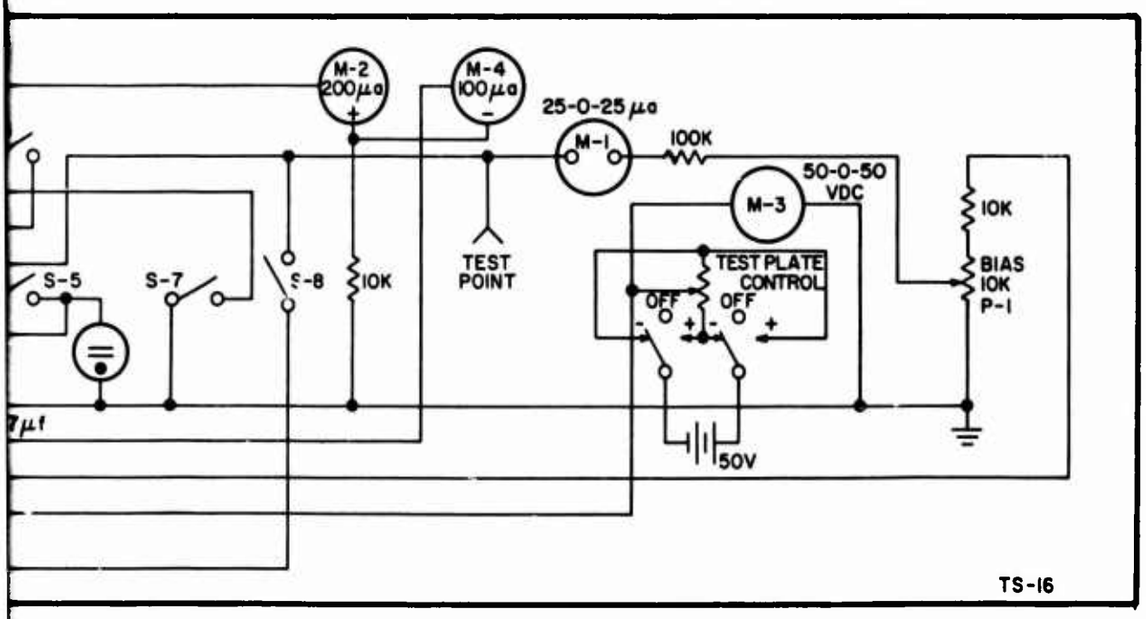
M-2
200μa
M-4
100μa
25-0-25 μa
M-1
100K
50-0-50
VDC
M-3
10K
S-5
S-7
S-8
10K
TEST
POINT
TEST PLATE
CONTROL
OFF
OFF
BIAS
10K
P-1
50V
TS-16

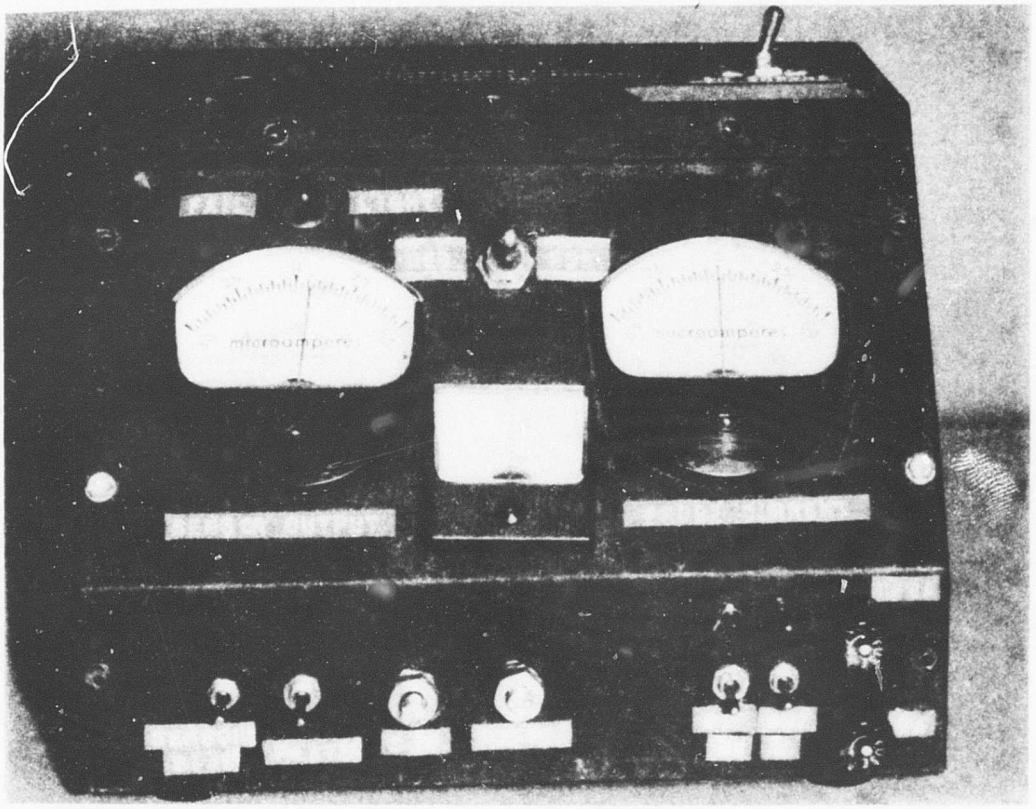

FIGURE 20. TS-16 DISCHARGER TEST SET

2. Test History and Results

The system did not function satisfactorily during the first test attempt, although bench testing had been satisfactorily performed. Investigation revealed that the CH-47 Chinook aircraft contained a nonstandard DC power supply. This power supply had a 2400 HZ semisinusoidal 4-volt ripple on the 24-volt supply, due to the aircraft DC supply being obtained from 400 HZ source through an unfiltered rectifier.

Further testing revealed a system oscillation caused by the detuning of the compensator circuit. The discharge system was removed from the aircraft and returned to the laboratory for modifications.

The problem with the DC ripple in the Chinook power supply resulted in circuit modifications of the D-03 Discharger System. The modifications provided a system that was able to operate under most adverse power supply conditions. In addition, the compensation network was modified as required to assure proper damping of the system.

The system was returned to Fort Rucker and reinstalled in the test aircraft. A ground check was performed by using the aircraft auxiliary power unit and adjusting the outputs for 28V DC $\pm$ 1V and 115 VAC $\pm$ 2V, 400 HZ $\pm$ 10 HZ. The availability of DC and AC power on the test panel inputs was verified.

AC power and DC power switches, as well as the switch on the cargo control unit, were turned on. The red (fail) light flashed momentarily; then the green (normal static energy level) light came on and the sensor motor began to operate.

The switch on the cargo control unit was turned off, the sensor motor stopped,and all system lights went out. The system was energized again by means of the switch on the pilot control unit, and the bias control on the test panel was adjusted for zero (on M-1, Figure 19).

The test plate control switch was turned to POS, and the test plate control was adjusted for a reading of +5 volts (on M-3, Figure 19). The test plate control switch was then flipped to NEG, and the test plate control was adjusted for a reading of -5 volts (on M-3). This sequence of plus and minus test plate adjustments was repeated for readings (on M-3) of 10, 15, 20, 25, 30, and 35 volts. The red (fail) light came on according to tolerances shown on the chart in Figure 21. The test plate control was then adjusted for zero, and the test plate control switch was turned off.

Proper fail light operation on the pilot and cargo control units was verified by turning off the AC power switch on the test panel. The red (fail) light came on and the green (normal static level) light went off on each of the two control units.

The DC power was turned off and the auxiliary power unit was shut down and removed from the vicinity of the aircraft. The test plate was removed from the sensor unit, and the drop line was attached by means of a battery cable clamp to an adequate grounding rod.

A sensor sensitivity test was performed with the aircraft on the ground as well as hovering at approximately 20 feet above the drop line ground rod. A chart recorder was connected to the test set and calibrated as discussed in the following paragraph.

Flight No. 1 (Figure 22a) showed the sensor monitor voltage change for a 400-volt potential change on the aircraft, when the aircraft was resting on the ground. Flight No. 2 (Figure 22b) showed the same relationship when the aircraft was hovering at approximately 20 feet altitude. The recorder sensitivity setting was 2 divisions/volt, or $\pm$10 volts full scale.

Consequently, the sensor sensitivity at ground and at 20 feet altitude can be determined to be as follows:

On the ground $\quad \theta_s = 1.25 \times 10^{-2} \dfrac{\text{Volts DC of Sensor}}{\text{Volts DC on Helicopter}}$

At 20 feet $\quad \theta_s = 0.625 \times 10^{-2} \dfrac{\text{Volts DC of Sensor}}{\text{Volts DC on Helicopter}}$

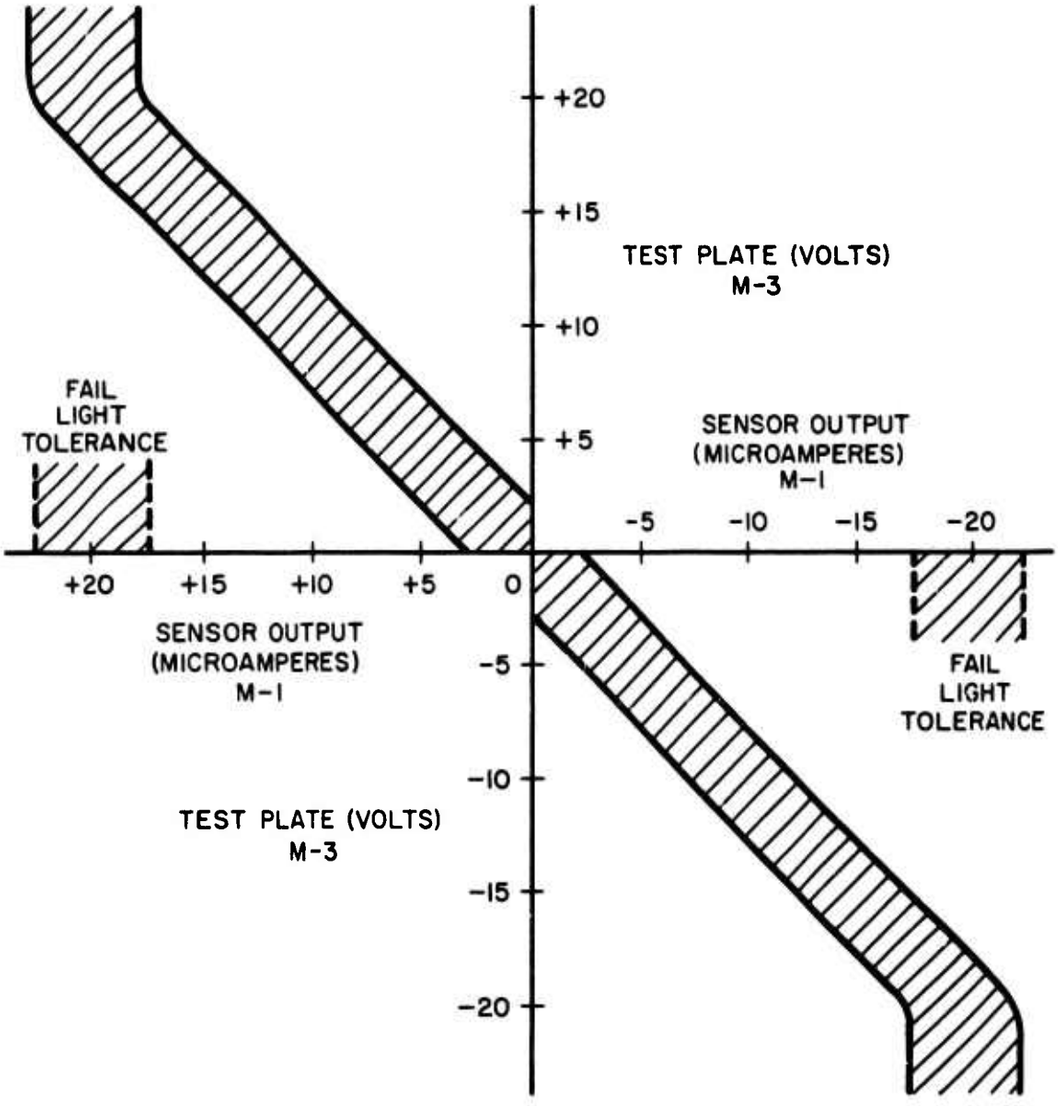

FIGURE 21. SYSTEM OPERATING PARAMETERS

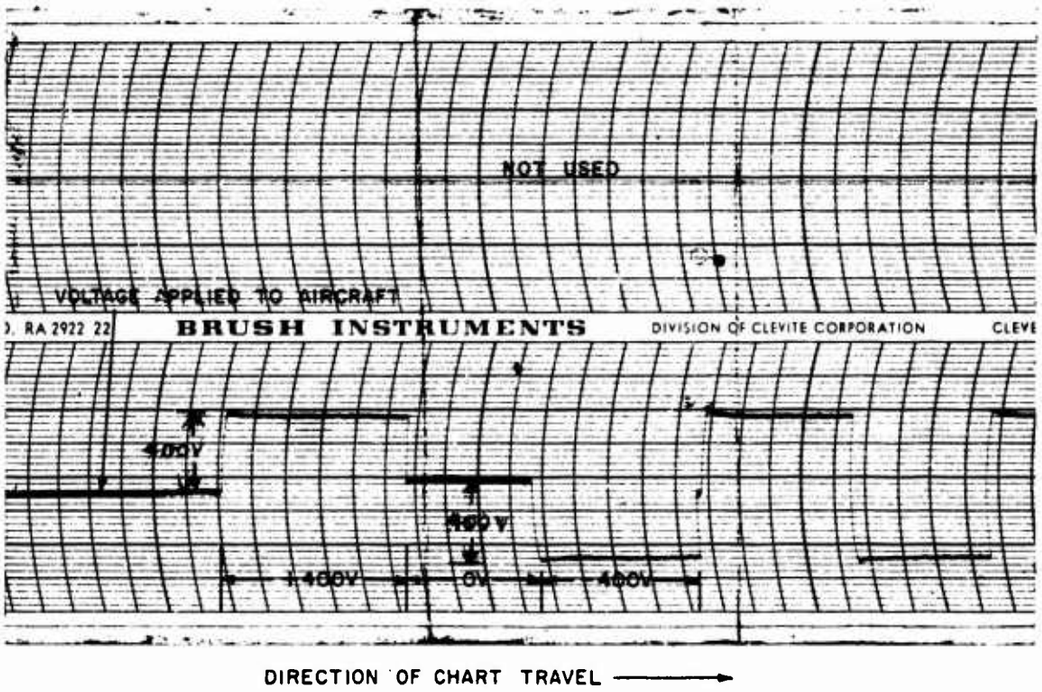

FIGURE 22a. FLIGHT TEST CHART RECORDING
SENSOR MONITOR VOLTAGE TEST, AIRCRAFT PARKED ON RAMP

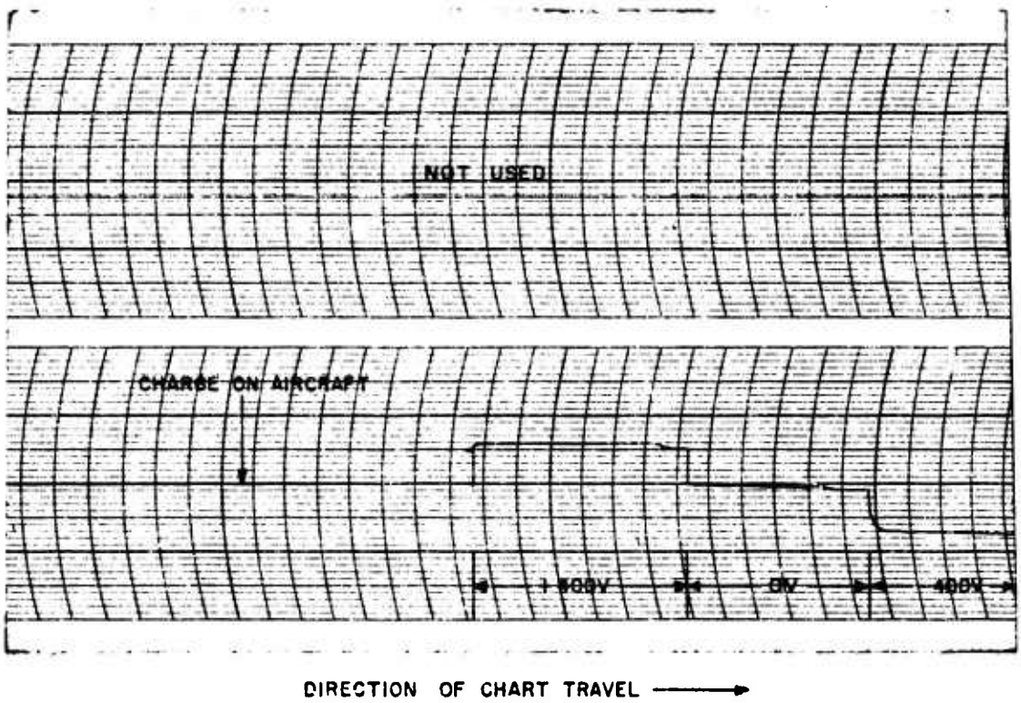

FIGURE 22b. FLIGHT TEST CHART RECORDING
SENSOR MONITOR VOLTAGE TEST, 20-FT ALTITUDE

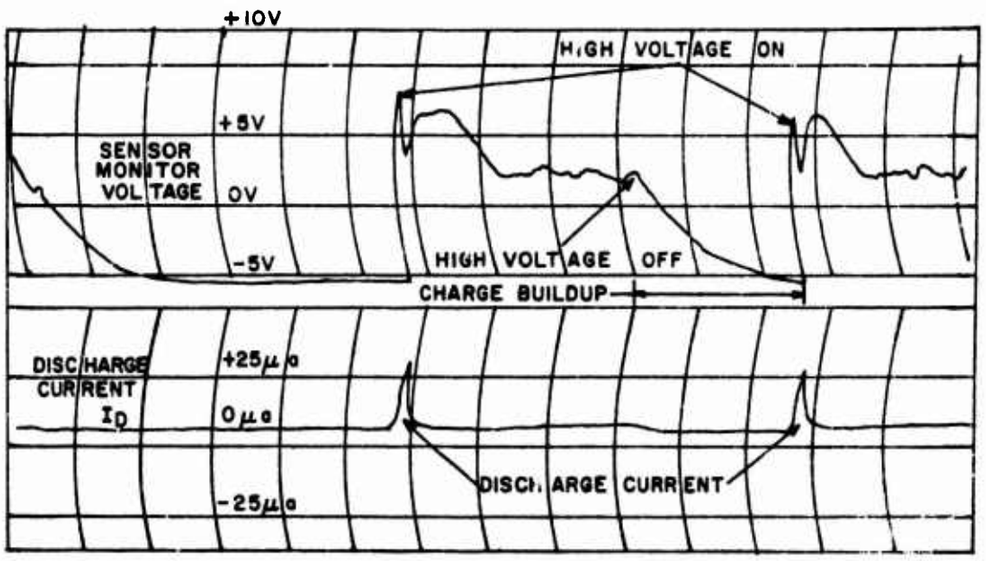

NOTE: 5MM IS 1 SECOND TIME

FIGURE 22c. FLIGHT TEST CHART RECORDING SYSTEM OPERATION TEST

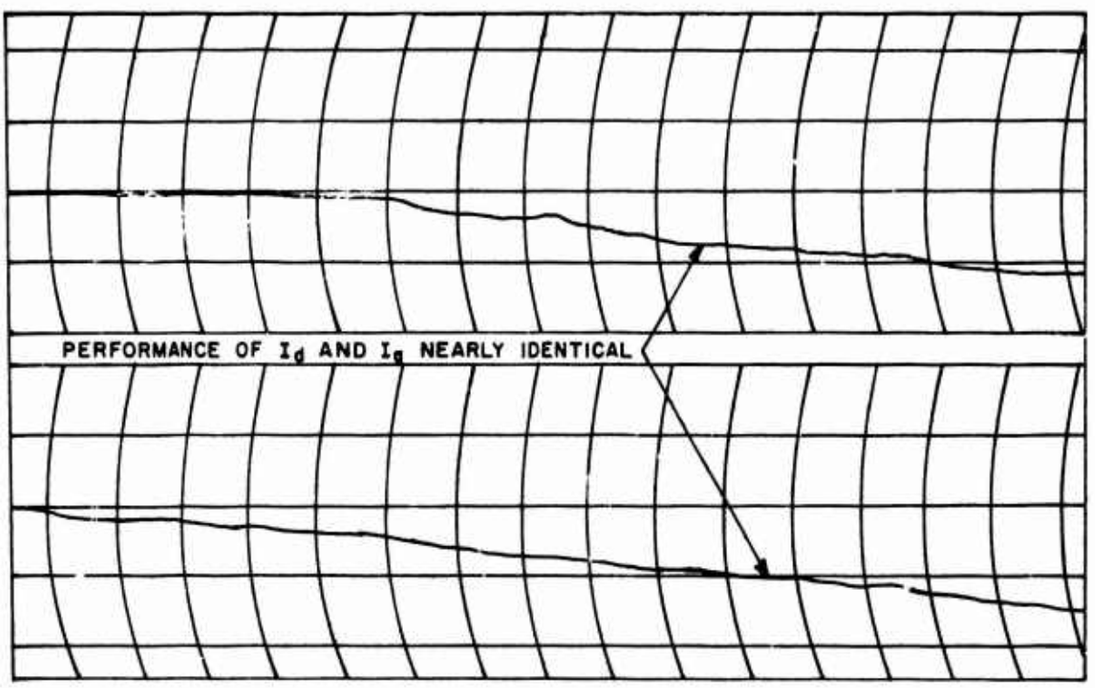

FIGURE 22d. FLIGHT TEST CHART RECORDING

Flight No. 3 (Figure 22c) was a test of the system operation in the air. The system high-voltage generators were deactivated to allow the aircraft to up static charge. This resulted in sensor monitor voltage saturation. At this point, the high-voltage generators were turned ON, and the probe current showed a transient as the charge was dissipated from the ship.

Flight No. 4 (Figure 22d) showed the system discharging capability and its recirculation characteristics. The two recording channels showed the current on the discharging probe (I_d) and the ground line (I_g) when the sensor was manually excited by using the test plate. The data obtained in this test show:

TABLE V

SYSTEM DISCHARGING CAPACITY AND RECIRCULATION

H.V.G. POLARITY	H.V.G. LOCATION	I_D PROBE CURRENT	I_G DROP LINE CURRENT
POSITIVE	RIGHT	+ 128 μA	+ 32 μA
NEGATIVE	LEFT	- 132 μA	- 22 μA

These data show the high level of recirculation current (I_D-I_G) exhibited by the system in its location on the CH-47 aircraft. This recirculation level is thought to be due to the presence of large conductive surfaces at the fuel tanks, located almost directly under the high-voltage generators.

3. Modifications as a Result of Tests

A new probe and high-voltage cable configuration was fabricated to allow repositioning of the probes at various locations with respect to the multiplier units. Subsequent flight tests indicated that the most efficient probe location was as a longitudinal extension of the multiplier units.

Circuit modifications to the discharger systems were made to correct the aforementioned Chinook power interface and system oscillation problems. A closed-loop simulation was performed to test the dynamic characteristics of the discharger system. The simulation approximated actual flight conditions as closely as possible.

B. FORT GREELEY, ALASKA

Flight tests at Fort Greeley were conducted to evaluate the discharger system under arctic conditions. These tests were performed during February 1964.

1. Test Setup and Procedures

Installation of the Discharger System for Fort Greeley flight testing was similar to that used in the Fort Rucker tests (see Figure 18). The discharge wicks, however, were mounted as a longitudinal extension to the multiplier units as was determined to be desirable in tests at Fort Rucker.

2. Test Results

Initial tests indicated the need for low-temperature compensation modifications. Low-temperature environmental tests had been conducted chronologically during the same period, and design changes determined in environmental tests were incorporated into the unit at Fort Greeley; the static electricity discharging system then operated satisfactorily.

The sensor sensitivity and system operation tests performed at Fort Greeley show results identical as those shown in Figure 22a, 22b, and 22c, as expected. Most of the effort at the arctic site was spent in an attempt to improve the recirculation characteristics of the system.

Special discharge probes were fabricated and used to determine the effect of the probe length on the recirculation level. The results are presented in Table VI.

The capability of the static electricity discharging system was demonstrated at the Fort Greeley site by contact between test personnel standing on the ground and the sling load cable suspended from the hovering CH-47 helicopter.

TABLE VI

EFFECT OF PROBE LENGTH ON RECIRCULATION LEVEL

Probe Length (in.)	Discharge Current $I_D(\mu a)$	Drop Line Current $I_G(\mu a)$	Recirculation Current $I_R=I_D-I_{GG}(\mu a)$	Recirculation Percent $\frac{I_R}{I_D}x100$
30	60	60	0	0
27	50	40	10	20%
24	60	25	35	58%

It must be noted that the longer probes, while being satisfactory in their recirculation characteristics, were not designed as permanent equipment from a structural standpoint. However, the results of these tests show the dependency of the recirculation level on the aircraft - probe geometry.

C. AIRCRAFT CAPACITANCE TESTS

Aircraft capacitance tests were performed both at Fort Rucker and at Fort Greeley. These tests were performed in accordance with the test procedure outlined on page 9 of TCREC Technical Report 62-33, Helicopter Static Electricity Discharging Device, 1962.

The results of these tests are presented in Figure 23.

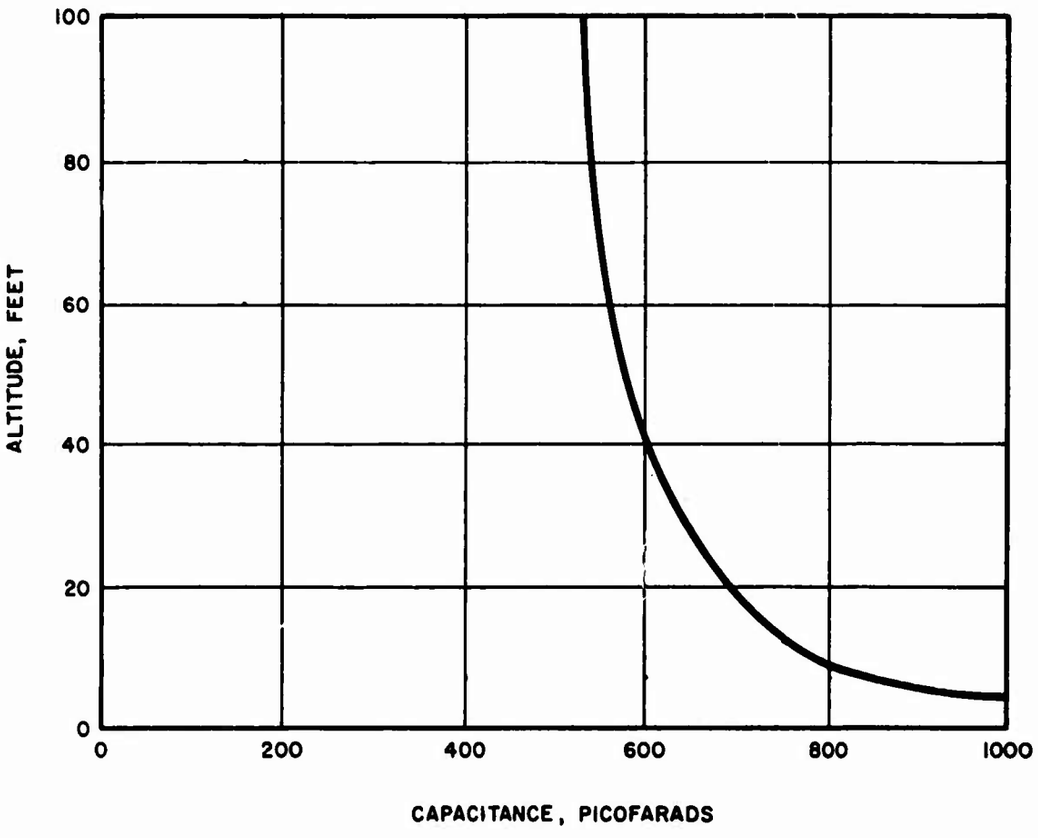

FIGURE 23. ELECTRICAL CAPACITANCE OF CH-47 HELICOPTER

CONCLUSIONS

The Model D-03 High Performance Active Electrostatic Discharger System satisfactorily dissipates the hazardous levels of energy present on tested helicopters. This performance was conclusively demonstrated by contact between an engineer on the ground and the sling load cable dropped from a hovering helicopter. Test data in the body of this report provide the documentation to substantiate the demonstrated performance.

RECOMMENDATIONS

Further investigation should be conducted to determine conclusively the maximum levels of electrostatic charges which may be built up on helicopters.

APPENDIX

TEST PROCEDURES

AEL PROJECT: 6401704

UNIT FOR TEST: Aircraft Static Electricity Discharge System

MANUFACTURER: Dynasciences Corporation
Fort Washington Industrial Park
Fort Washington, Pennsylvania

P.O. No.: 899

GOV'T CONTRACT: DA 44-177-AMC-114(T)

I. OPERATION

The system will be checked for proper operation using the following operational procedure:

1. Make all connections as shown on the attached interconnection diagram. (Refer to Figure 24.)

2. Connect system to 115V, 400 HZ and 28V DC power sources.

3. Turn on 115V, 400 HZ and 28V DC switches on test panel.

4. Turn on static discharge system with switch on either control box.

5. Turn switch on test panel from ON GROUND to IN AIR position.

6. Apply -22.5V DC to test plate on sensor unit. Meters on test panel should read:

   a. Helicopter Charge - 18μa ($\geq$ 900 on meter)
   b. Negative Output - 140μa
   c. Positive Output - 100μa

7. Apply +22.5V DC to test plate on sensor unit. Meters on test panel should read:

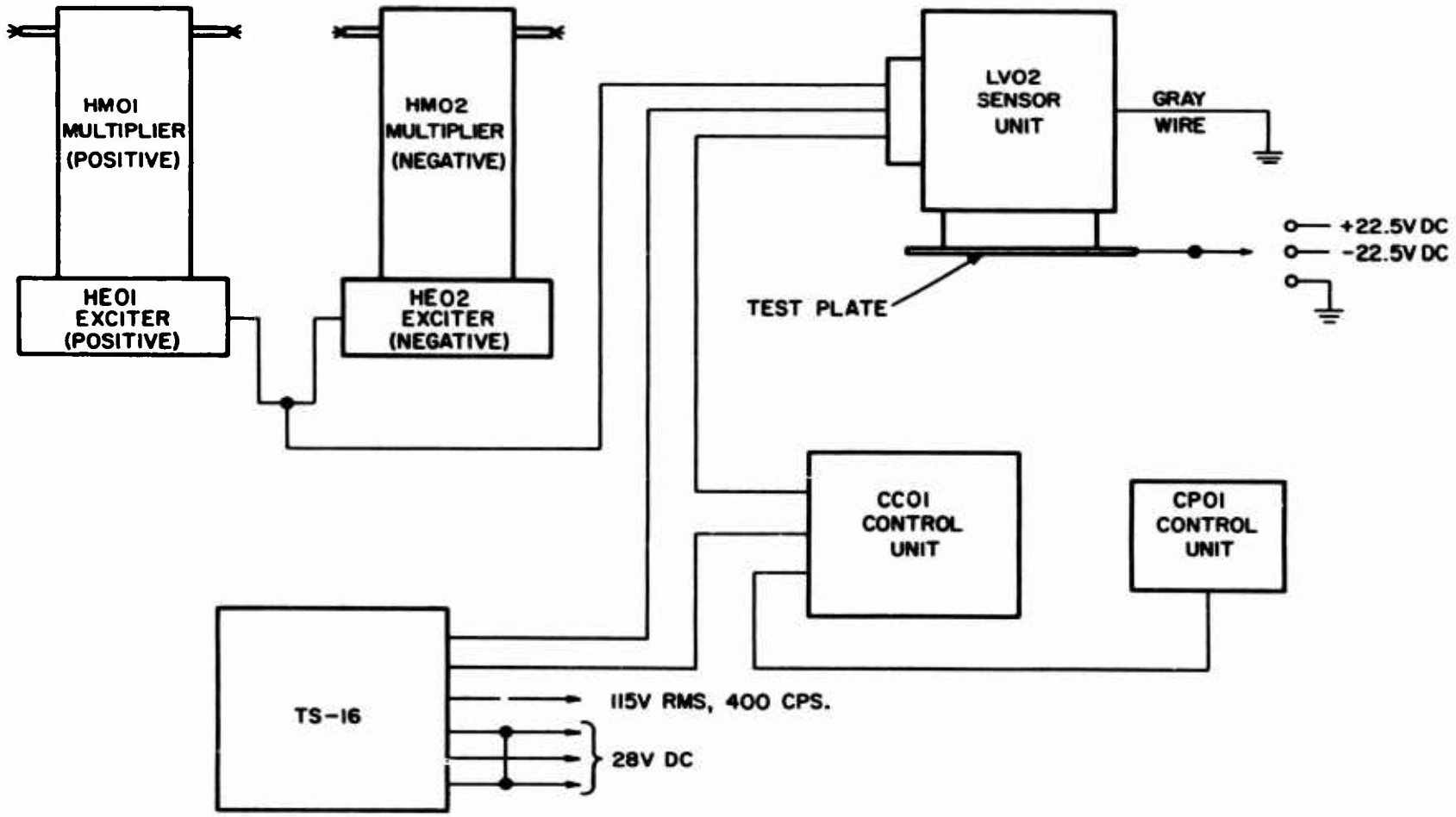

FIGURE 24. ENVIRONMENTAL TEST SETUP

a. Helicopter Charge - 18 μa (≥ 900 on meter)
b. Negative Output - 100 μa
c. Positive Output - 140 μa

8. Connect ground strap or lead to test plate on sensor unit. Meters on test panel should read:

a. Helicopter Charge - 5 μa (≥ 250 on meter)
b. Negative Output - 40 μa
c. Positive Output - 40 μa

When energizing the system, the operator should ground himself by holding onto conduit, the test panel or any "earth ground" to prevent electrical shock. Warning should be given to others in the general test area.

II. ENVIRONMENTAL TESTS

The system will be subjected to the following environmental tests in the order listed. All tests will be performed in accordance with Military Specification MIL-E-5272C. Before and after each test (during, where required), the system will be operated in accordance with I, above.

Where possible, all units of the system will be subjected to the tests at the same time. Otherwise, individual units will be tested but connected electrically and operating where required.

1. Low Temperature
2. Vibration
3. Shock
4. Explosion
5. High Temperature
6. Altitude
7. Temperature & Altitude
8. Acceleration
9. Humidity
10. Sand & Dust (dust velocity - 2500 ft/min)
11. Rain
12. Fungus
13. Salt Spray (external parts & structural assemblies only)

Unclassified

Security Classification

DOCUMENT CONTROL DATA - R & D

(Security classification of title, body of abstract and indexing annotation must be entered when the overall report is classified)

1. ORIGINATING ACTIVITY (Corporate author) Dynasciences Corporation Blue Bell, Pennsylvania	2a. REPORT SECURITY CLASSIFICATION Unclassified 2b. GROUP

3. REPORT TITLE

Fabrication and Testing of an Active Electrostatic Discharger System for the CH-47 Helicopter

4. DESCRIPTIVE NOTES (Type of report and inclusive dates)

Final Technical Report

5. AUTHOR(S) (First name, middle initial, last name)

Juan de la Cierva
David B. Fraser
Paul B. Wilson, Jr.

6. REPORT DATE October 1967	7a. TOTAL NO. OF PAGES 63	7b. NO. OF REFS
8a. CONTRACT OR GRANT NO. DA 44-177-AMC-114(T) b. PROJECT NO. Task 1F121401A14130 c. d.	9a. ORIGINATOR'S REPORT NUMBER(S) USAAVLABS Technical Report 67-60 9b. OTHER REPORT NO(S) (Any other numbers that may be assigned this report) DCR 224B	

10. DISTRIBUTION STATEMENT

This document has been approved for public release and sale; its distribution is unlimited.

11. SUPPLEMENTARY NOTES	12. SPONSORING MILITARY ACTIVITY U.S. Army Aviation Materiel Laboratories Fort Eustis, Virginia

13. ABSTRACT

Numerous incidents of severe shock to ground personnel and potential hazards to cargo during external sling load cargo operations have led to extensive research efforts by the U. S. Army Aviation Materiel Laboratories aimed at the dissipation of high electrostatic energy levels present on helicopters. Dynasciences Corporation, in cooperation with USAAVLABS, has fabricated and tested an active electrostatic discharging system for the CH-47 helicopter.

The Model D-03 Electrostatic Discharger is essentially a closed-loop servo system. This report covers its fabrication, mechanical evaluation, environmental testing, and flight testing under both arctic and dusty/high-humidity conditions. Drawings and photographs are included in the report as an aid to a thorough understanding of the system.

DD FORM 1 NOV 68 1473 REPLACES DD FORM 1473, 1 JAN 64, WHICH IS OBSOLETE FOR ARMY USE.

Unclassified

Security Classification

14. KEY WORDS	LINK A		LINK B		LINK C	
	ROLE	WT	ROLE	WT	ROLE	WT
Electrostatics Electrostatic Dissipation Electrostatic Discharge CH-47 Helicopter						